Doctoral Dissertation
Doctoral Program in Bioengineering and Medical Surgical Sciences (37th Cycle)

Magnetic Resonance Imaging - Guided Cardiac Catheterization in Children and Patients with Congenital Heart Disease

Enrico Piccinelli

* * * * * *

Supervisors
Prof. Marco Agostino Deriu, Supervisor
Prof. Gianfranco Butera, Co-Supervisor

Doctoral Examination Committee:
Prof. Petru Liuba
Prof. Thomas Krasemann

Politecnico di Torino
April 1st, 2025

I hereby declare that, the contents and organisation of this dissertation constitute my own original work and does not compromise in any way the rights of third parties, including those relating to the security of personal data.

.....

Enrico Piccinelli

Rome, April 1st, 2025

Summary

Background: Magnetic Resonance Imaging (MRI)-guided catheterization combines the benefit of cardiac catheterization with the advantages of cardiovascular magnetic resonance (CMR), allowing simultaneous haemodynamic assessment, detailed tissue characterization and anatomical evaluation without the use of ionising radiation. Real-time CMR guides catheter navigation through the heart chambers and vessels allowing haemodynamic and flow assessment under the same sedation or anaesthesia conditions. The drawback is the slightly increased procedural complexity due to the scarce availability of dedicated MRI-conditional catheters and wires. We retrospectively report our experience of MRI-guided catheterization in children and patients with congenital heart disease (CHD), comparing the cardiac output and indexed pulmonary vascular resistance measured using the traditional Fick method and CMR flows under the same haemodynamic conditions.

Methods: Children and young adults affected by CHD or cardiomyopathy referred for cardiac catheterization and MRI between May 2022 and October 2024 were invited to undergo MRI-guided heart catheterization. All MRI-guided catheterizations were performed in a suite equipped with a 1.5-Tesla MRI scanner adjacent to a preparation room at Ospedale Pediatrico Bambino Gesù in Rome. Baseline demographics, clinical characteristics, procedural data, invasive hemodynamic findings, CMR flows and procedural complications were recorded. Procedural success was defined as the completion of a full right heart catheterization. All procedures were performed by one of two paediatric interventional cardiologists with more than five years of experience in X-Ray-guided catheterization. Systemic and pulmonary blood flows were obtained by phase contrast CMR and compared to the Fick principle. QP:Qs and indexed pulmonary vascular resistance were also compared.

Results: Twenty-five patients underwent MRI-guided heart catheterization. The mean age was 12.3 ± 11.1 years old and the mean weight was 35.7 ± 22.5 Kg. Most of the patients had a cardiomyopathy and the indication for catheterization was surveillance and/or placement on the heart transplant list (n = 13; 52%), seven patients were univentricular heart palliated with Glenn (n =2) and Fontan (n = 5), tricuspid valve anomalies (n =1), total anomalous pulmonary venous return post-repair (n =1), double outlet right ventricle post-repair (n =1), Uhl's anomaly (n =1) and congenitally corrected transposition of great arteries palliated with

pulmonary artery banding (n =1). A complete MRI-guided cardiac catheterization was performed successfully in 96% of patients. Most procedures were performed from a femoral access (n = 23; 92%). There were no procedural complications related to the procedure and no patient experienced hemodynamic instability or needed resuscitation. There was a moderate correlation between cardiac and pulmonary index measured by the Fick method and CMR flows (R^2 0.59, $p < .001$ and R^2 0.42; $p < .001$ respectively). There was a strong correlation between indexed pulmonary vascular resistance measured by the Fick method and CMR flows (R^2 0.86; $p < .001$) with a mean difference of -0.23 ± 0.51 WU*m^2, 95% CI -1.23 to 0.76 WU*m^2.

Conclusions: MRI-guided catheterization is feasible and safe in children and patients with CHD and can be performed with standard technology using existent CMR scans. MRI combines a better soft tissue visualisation with additional haemodynamic information obtained by catheterization, without the use of X-Ray. Flow measurements and pulmonary vascular resistance obtained by CMR flows and with the traditional Fick method have a good correlation at the baseline condition. Advancements in MRI technology with improved image quality, faster scanning times, and dedicated catheterization equipment may increase the role of MRI-guided catheterization in CHD and open more space for interventional procedures.

Acknowledgment

I would like to express my sincere and deepest gratitude to my supervisor, Prof. Marco Agostino Deriu, and co-supervisors, Prof. Gianfranco Butera and Prof. Lorenzo Galletti for their continuous and invaluable guidance, support, and mentorship throughout my PhD journey. A heartfelt thanks for the unique opportunity they provided to me as early-stage researchers of the PremAtuRe nEwborn motor and cogNitive impairmenTs (PARENT) Project, which allowed me to learn from professionals of different backgrounds, fundamental in my interventional and academic development.

I'm truly grateful to my interventional cardiology colleagues at Ospedale Paediatrico Bambino Gesù. First of all, the Head of the cath lab Gianfranco Butera for believing in my human, professional and research potential, investing in my development and challenging my capacities. His forward-thinking approach has played a crucial role in my early career as a young interventional cardiologist and researcher. I would like to express my profound gratitude also to my colleagues Mara Pilati and Micol Rebonato for their daily support and trust who have been essential in letting me develop my academic interest while sharing their clinical and interventional experience. The interventional team's inclination to engage openly, share expertise, and support each other is the true key to the success of our daily activity.

I would like to acknowledge the PARENT Project supervisors, in particular Prof Marco Deriu, for their enthusiasm in managing the project and putting together researchers with totally different backgrounds. The events, meetings, conferences and activities that were organised challenged me to develop critical skills and think out of the box with a multidisciplinary approach. These have been years of enormous human and academic growth and I feel extremely thankful to have been part of the project together with the other early-stage researchers. I learned from all of them, thanks to interdisciplinary perspectives, which enriched my journey. A special thanks to my PARENT ESR colleagues and now friends Pablo Romero, Konstantinos Panagiotopoulos and Syed Taimoor Hussain Shah for the incredible journey together.

I would like to sincerely thank the multidisciplinary team that initiated and supported the development of the MRI-guided cardiac catheterization program. My deepest gratitude goes to Dr. Gianfranco Butera and Dr. Micol Rebonato for their outstanding leadership, clinical vision, and unwavering support throughout this journey. I am also profoundly grateful to the dedicated teams of anesthesiologists, technicians, and nurses, whose expertise, commitment, and collaborative spirit were essential in making this innovative approach a reality.

A heartfelt thanks to the Advanced Cardiothoracic Imaging Unit of Ospedale Paediatrico Bambino Gesù led by Aurelio Secinaro for their expertise and willingness to collaborate on different clinical research activities. A special thanks to Veronica Bordonaro, Davide Curione and Alessandra Marasi who were essential in the development of this and other projects.

I would like to thanks the PoliTO Department of Mechanical and Aerospace Engineering for their collaboration on many projects in these three years, in particular Prof Umberto Morbiducci, Karol Calò and Valentina Mazzei for their extremely valuable expertise in 4D flow MRI and fluid-dynamics.

I extend my sincere thanks to the Boston Children's Hospital and Deutsches Herzzentrum München colleagues who hosted me during my PhD abroad periods and share with me their knowledge and vision. Their collaboration in exploring various aspects of interventional cardiology have significantly enriched my research and professional experience.

I would like to dedicate this thesis to my loving Family

Whose unwavering support and love have been my foundation; to my loving and caring wife Francesca, for her patience and encouragement and my little daughter Bianca for her pure and beautiful smile. To my dear parents and brother who have been the columns of my life and inspiration.

To my dear friends, who have been pillars of strength; to my supervisors Gianfranco Butera and Marco Agostino Deriu, for their invaluable guidance; and my colleagues Micol Rebonato, Mara Pilati and Lisa Bianco for their precious support and inspiration..”

Contents

Chapter 1

Advancement in the diagnosis of congenital heart diseases

1.1 Background

The worldwide prevalence of congenital heart disease (CHD) is approximately 8-9 per 1000 newborns. (1-4) Advances in diagnosis, interventional and surgical management have dramatically improved the outcome for children born with CHD with more than 90% surviving into adulthood. (3,5) Diagnostic work-up for patients with CHD includes medical history with detailed information about previous surgeries and interventions, clinical evaluation and examination, electrocardiogram and pulse oximetry. Non-invasive imaging is routinely performed by transthoracic echocardiography, while transoesophageal echocardiography and cardiovascular magnetic resonance (CMR) imaging are performed only where indicated.

CMR has emerged as an important diagnostic tool for patients with CHD. Nowadays, it is the gold standard for the quantification of volumes, heart valve disease, shunts and collaterals, right ventricular size and function in patients with pulmonary regurgitation, complex CHD such as univentricular heart and complex aortic arch abnormalities. (6-8) Moreover, the absence of ionising radiation makes CMR a useful tool when serial evaluations are needed, for example for monitoring aortic dimensions. (3) It provides high-quality soft-tissue visualization, 3-dimensional anatomic reconstruction and myocardial tissue characterisation. (9,10) Finally, it allows systemic and pulmonary blood flow calculation, which is very useful in patients with multiple sources of blood supply.

Cardiac catheterization has a central role in the diagnosis and surgical risk stratification of patients with CHD, pulmonary vascular disease, cardiomyopathy, and heart failure. There are various indications for performing a diagnostic catheterization, including shunt quantification, pressure gradients, evaluation of systemic-pulmonary collaterals, discrimination between constrictive and

restrictive physiology etc.. Furthermore, cardiac catheterization represents the gold standard for the diagnosis and classification of pulmonary hypertension which is often encountered in patients with CHD (11) In this setting cardiac catheterization includes vasoreactivity testing, which plays a crucial role in the shunt closure decision-making. Usually, the Fick principle is used to quantify flow and calculate PVR. This method is based on oxygen consumption assumption and relies on multiple measurements. Cardiac catheterization is performed with X-ray guidance which exposes patients, who often require many catheterizations during their life, to the risks correlated to ionising radiation. The imaging guidance is suboptimal because radiopaque wires, catheters, balloons and devices are visualised within the patient cardiac silhouette and vessels, having as markers other thoracic structures such as bones, trachea and bronchi. Moreover, the heart chambers and vessels can be depicted only by injection of iodinated contrast with poor soft tissue definition (12) Interventional cardiologists working with fluoroscopy make assumptions which sometimes do not reflect the true anatomy.

1.2 Pulmonary hypertension

Pulmonary hypertension (PH) is a pathophysiological disorder involving multiple clinical conditions and is defined by a mean pulmonary arterial pressure (mPAP) >20 mmHg at rest. It may be associated with various respiratory and cardiovascular diseases (11) In the last decades enormous progress has been made in the diagnosis, management and treatment of patients suffering from pulmonary hypertension, in the direction of a multidisciplinary approach with a team of experts. (13-16) The 2022 ESC/ERS Guidelines for the diagnosis and treatment of pulmonary hypertension classified PH according to the clinical condition associated with PH, which shares similar pathophysiology, clinical presentation and management. (11) Schematically ESC/ERS Guidelines divided patients with PH in five groups:

GROUP 1 Pulmonary arterial hypertension (PAH)

GROUP 2 PH associated with left heart disease

GROUP 3 PH associated with lung diseases and/or hypoxia

GROUP 4 PH associated with pulmonary artery obstructions

GROUP 5 PH with unclear and/or multifactorial mechanisms

One of the most important aspects of this condition is defining the haemodynamic characteristics of PH by obtaining the pulmonary artery wedge pressure (PAWP) and the pulmonary vascular resistance (PVR). This is crucial in the definition of pre-capillary and post-capillary PH, to distinguish increased pulmonary pressures due to a true pulmonary vascular disease, PH associated with left heart disease or other conditions. A threshold of PAWP ≤15 mmHg is considered the discriminant for pre-capillary PH and the upper limit of normal PVR is 2 Wood units (WU). (17-19) However, patients may suffer from combined post- and pre-capillary pulmonary hypertension which together contribute to elevation in pulmonary artery pressure.

Pre-capillary PH: mPAP >20 mmHg, PAWP ≤15 mmHg, PVR >2 WU

Post-capillary PH: mPAP >20 mmHg, PAWP >15 mmHg, PVR ≤2 WU

Combined post- and pre-capillary PH: mPAP >20 mmHg, PAWP >15 mmHg, PVR >2 WU

1.2.1 Pulmonary hypertension in congenital heart disease

Pulmonary hypertension in adults with CHD is estimated between 3–7% and includes a very heterogeneous population. (3,11,20) It can occur in males and females but it is more frequent in the latter and increases with time from the defect repair. (21,22) The scenario can vary from PH with small/coincidental defects, PH associated with prevalent systemic-to-pulmonary shunts, PH after surgical or interventional correction and Eisenmenger syndrome. (11,22-24)

The increased PVR in this population is often due to a multifactorial obstructive pulmonary vasculopathy and it is important to distinguish this PH-CHD condition (classified in group 1 ESC/ERS Guidelines) from post-capillary PH in groups 2 and 5 of the same classification. (3) Moreover, patients with CHD may have segmental PH with high variability in the hypertensive pulmonary vascular bed, as seen in subjects with pulmonary atresia with ventricular septal defect and major aortopulmonary collateral arteries. PH is a significant prognostic factor in patients with CHD, impacting the clinical status and outcome of this rapidly growing population. (25) It requires particular attention in pregnancy and before surgical repair. (26)

The diagnosis of PH in patients with CHD incorporates a complex work-up including patient history, examination, laboratory tests, imaging and lung function tests. Right heart catheterization remains the gold standard to assess the necessity of starting a vasodilator therapy in patients with pulmonary vascular disease and suitability for surgical or interventional repair. (3) Fontan circulation is also sometimes associated with pulmonary vascular disease and elevated PVR. High pulmonary artery pressure in these patients is generally caused by increased ventricular filling pressure associated or not with significant atrioventricular valve regurgitation. (3) PVR can be calculated using the formula (mPAP– PCWP) / Qp and its value and the response to vasoreactivity test with nitric oxide (NO) and/or oxygen is useful information for decision-making. In most catheterization laboratories the Fick principle is used to quantify flow. It depends on multiple measurements such as haemoglobin values, oxygen saturations, partial pressures and oxygen consumption, increasing the chance of inaccuracy. (27,28)

1.3 X-Ray guided catheterization exposure risks

Cardiac catheterization is performed with X-ray guidance which exposes patients and operators to the risks correlated to ionising radiation. (29) Despite the reduction in radiation exposure over the years, the risk for infants and children often requiring multiple long procedures remains not negligible. Indeed, children are more radiosensitive than adults, exposing them to radiation-induced chromosomal damage, increasing the risk of developing cancer, also because live longer to experience radiation effects (29-33) In many centers, patients after heart transplants need annual surveillance cardiac catheterizations and sometimes frequent endomyocardial biopsies. Children with CHD and after heart transplant are the ones who benefit more from MRI-guided catheterization, sparing radiation and getting at the same time haemodynamic data and CMR information about possible myocardial rejection and perfusion abnormalities from cardiac allograft vasculopathy. (34) Moreover, operators are exposed to the risks correlated to X-Ray and chronic orthopaedic injuries due to the use of lead, worn as protection from radiation.

Chapter 2

MRI-guided catheterization

2.1 Background

Razavi R et al, first described a novel method of cardiac catheterization guided by MRI with radiographic support in 2003. (35) MRI-guided catheterization combines the benefit of cardiac catheterization with the advantages of CMR, allowing simultaneous haemodynamic assessment, detailed tissue characterization and anatomical evaluation without the use of ionising radiation.
The drawback is the slightly increased procedural complexity due to the reduced spatial and temporal resolution and the scarce availability of dedicated MRI-conditional catheters and wires. (32) Anyway, right heart catheterization under CMR guidance can be generally performed and all chambers and vessels of interest can be accessed. (34,36,37) In preliminary experiences transfemoral right heart catheterization was performed first under X-ray and then under continuous real-time MRI guidance. (36) Ratnayaka K et al, systematically compared patients undergoing right heart catheterization under CMR and X-Ray fluoroscopy guidance, finding similar procedural time including catheter manipulation, pressure recording and oximetry. Gadolinium-filled balloons visualised under MR were more successful than X-Rays in entering the left pulmonary artery. (36)

The added value of MRI-guided catheterization is the soft tissue visualisation which helps the cardiologist in understanding the catheter position within the heart and vessels. Pressures and saturations obtained during the procedure are combined with flow data obtained from CMR, allowing the calculation of shunts and resistances. An unlimited number of image planes can be obtained with improvement in the accuracy of catheter manipulation, which is particularly important in children and patients with CHD. (38)

There are two different methods of visualisation of CMR catheter devices: passive and active.
- Passive tracking: Passive visualization refers to intrinsic equipment properties such as a small amount of metal or balloon wedge catheters filled with air or gadolinium which generates magnetic susceptibility artefacts or signal voids.

Passive tracking is effective when it reaches a compromise between enough signal void without losing soft tissue definition. Artefacts are proportional to the magnetic susceptibility of the materials and passive tracking takes place with normal imaging with no special processing required (32,39,40) Differentiation from nearby tissue is difficult with passive tracking and it is often impossible to see catheters in their entirety length without many changes in plane images. Passive tracking requires that the device is confined within the selected imaging slice. (37) However, with this strategy there is no need for an intravascular coil that increases catheter diameter, reducing the accessibility of small vessels in younger children. (41)

- Active tracking: Active guidewires and catheters are visualized by using miniature radiofrequency coils or electronic components connected to the CMR scanner. These devices emit or receive a signal to identify their location. The electronic component position can then be superimposed on an acquired roadmap image in real-time to allow direct visualization. It requires post-processing and its clinical use is limited. (39,40,42-46) This strategy allows the device to be always visualized even outside the selected imaging slice. (37)

2.2 Rationale of MRI-guided cardiac catheterization

The rationale of MRI-guided cardiac catheterization is combining advanced imaging, hemodynamics assessment and potential intervention in a single radiation-free procedure. (47) Many advantages make this relatively new technique appealing especially in the CHD field:

- MRI provides a better soft tissue visualisation, allowing to define the intracardiac anatomy and its properties such as edema, fibrosis etc. This is extremely important in CHD due to the complexity of anatomies and their variation after cardiac surgery. (37,48,49)
- MRI provides important additional haemodynamic information such as flow analysis, regurgitation analysis, chamber volumes and mass. These parameters together with the standard haemodynamics obtained by catheterization offer a potential improvement in decision-making.
- MRI-guided cardiac catheterization provides accurate haemodynamic information without the use of X-Ray, reducing the risks associated with ionising radiation for patients and operators. (29,31,35,50)
- Reduce the anaesthesia time by obtaining the haemodynamic and flow data under the same conditions.
- Early detection of complications such as bleeding due to continuous visualization. (51)

In the last years there was an improvement in image resolution due to more powerful magnets and effective management of respiratory and cardiac motion artefacts. (39) Moreover, procedural times, despite an initial learning curve, are almost comparable to traditional X-ray guided cardiac catheterization, also because image acquisition times have improved.

2.3 Hemodynamic evaluation by MRI-guided cardiac catheterization

Catheterization measurements of cardiac output and pulmonary vascular resistance are historically made by using the Fick method or thermodilution which are subject to errors from intrinsic inaccuracy or imprecise assumptions. (52) The Fick method is based on oxygen consumption (VO2) which is laborious to measure so in most catheterization laboratories assumptions are made using the LaFarge-Miettinen formula, which is based on body surface area (BSA), age, and heart rate. (53) VO2 direct measurement is infrequent in clinical practice. These calculations are affected by many factors such as anaesthesia, VO2 variations in different hemodynamic conditions, spontaneous fluctuation, difficult simultaneous blood sampling and multiple sources of pulmonary blood flow. (54,55)
Furthermore, the Fick method is not accurate in patients with large intracardiac shunt and high pulmonary blood flow due to reduced pulmonary arteriovenous oxygen content difference. For the same reason, a pulmonary vasodilation test with high-concentration oxygen further reduces the accuracy of this principle. (28)
The thermodilution technique is also not precise in patients with intracardiac shunts, significant valvular regurgitation and low flow states. (37)

Velocity-encoded phase-contrast magnetic resonance is an established method to quantify blood flow and Qp:Qs assessment have also been proved accurate. (56-58) Comparison of flows and resistances between Fick and CMR flows had controversial results. Preliminary studies in swine and humans demonstrated a good correlation between the calculation of flows and pulmonary vascular resistance. (35,59) Other Authors suggest that CMR flow data quality is better than traditional measurement by the Fick method or thermodilution. (51,60)

In 2004, Muthurangu V et performed MRI-guided cardiac catheterization in twenty-four children and adults with suspected PH or CHD requiring pre-surgical assessment of PVR. They found a good correlation between basal PVR calculated by the Fick method and MRI-derived blood flows. However, they found a poor correlation when PVR was also calculated at 20 ppm nitric oxide and 30% or 100% oxygen. (28)

Ratnayaka et al performed a right heart catheterization under CMR guidance in 50 children and found slightly higher pulmonary and systemic blood flow when measured with the Fick principle compared with ones derived from CMR. They

included children post-heart transplant, simple shunts, pulmonary hypertension, cardiomyopathy, valvular and heart disease. (34)

Rogers T et al reported the Bethesda experience of MRI-guided right heart catheterization in 102 patients, comparing cardiac output and pulmonary vascular resistance obtained by CMR flow versus Fick, under resting conditions and after pulmonary vasoreactivity test with inhaled nitric oxide and oxygen. They demonstrated an excellent agreement at baseline catheterization on room air. There was a reasonable agreement during the vasoreactivity test with inhaled 100% oxygen and 40 ppm nitric oxide, which is less precise because of reduced arteriovenous oxygen difference. (52) Rogers T et al reported a stronger correlation on the vasoreactivity test than Muthurangu et al (28), speculating that this result could be explained by the higher number of paired calculations, use of estimated VO2 and lower mean PVRi at baseline. (52)

Theoretically, hemodynamic evaluation by MRI-guided catheterization, and coupling invasive pressure measurement with MRI-derived blood flows should provide a more accurate hemodynamic assessment. Stroke volume and pulmonary or systemic cardiac output can be measured by volumetric analysis of cardiac function or by MRI phase-contrast flow techniques. Then, intracardiac shunts (Qp:Qs) can be calculated from the pulmonary artery and aortic flows and pulmonary vascular resistance can be obtained from MRI flows and catheterization pressures. (37)

2.4 MRI-guided cardiac catheterization in pregnancy

MRI-guided catheterization can be an excellent alternative also in pregnant women, avoiding ionising radiation and its known adverse effects on the fetus. Tzifa A et al described the case of a 33-year-old woman with recently diagnosed complex CHD and severe pulmonary hypertension who underwent an MRI cath to confirm the diagnosis and assess pulmonary arterial pressure and pulmonary vascular resistance, to stratify the risk of her pregnancy. (61) Pulmonary vascular disease is associated with a 40% risk of maternal death or heart failure, making the haemodynamic assessment crucial for risk stratification, consultation and therapy. (62)

2.5 MRI-guided cardiac catheterization feasibility

MRI-guided diagnostic catheterization is usually completed with no need for bailout catheterization under fluoroscopy. This procedure is feasible in adult and children affected by many conditions, with bientricular and univentricular heart. (34,35,52) Some technical aspects should be considered in case of post-surgical repair anatomy, pulmonary hypertension and/or severe tricuspid valve regurgitation.

Rogers T and al failed to reach the pulmonary artery with a balloon wedge pressure catheter only in 5 patients out of 102 patients because of severely dilated right heart chambers caused by pulmonary hypertension. Anyway, reaching the pulmonary arteries in the same patients was unsuccessful also under fluoroscopy guidance without the help of a guidewire. (52)

Ratnayaka K et al safely completed MRI-guided catheterization without a guidewire in 15 to 16 adult patients with or without CHD, being unsuccessful only in one patient with a large secundum ASD, dilated pulmonary arteries and moderate pulmonary artery hypertension. (36) The procedure can be challenging in patients with CHD as described by Velasco Forte et al who cannot successfully perform it in 4 out of 30 patients due to the need for unavailable guidewire in a patient with a criss-cross heart, pulmonary hypertensive crisis in another and the artefact caused by pulmonary artery stents in two patients with single ventricle circulation. (63) MRI-guided catheterization is generally feasible in patients with single ventricle anatomy status post Glenn or Fontan. Sometimes, a wire is needed to cross the conduit fenestration to assess atrial and ventricular pressures. (63) Another challenge that can limit the feasibility of catheterization in CMR is the difficulty in reaching patients' groin access inside the scanner and manipulating catheters and wires in small children.

Knight DS et al, focused their attention on determining the predictors of procedure success, failure and duration in patients with pulmonary artery hypertension. They enrolled fifty patients who underwent MRI-guided right heart catheterization and could complete the procedure in forty-seven patients. Higher mean pulmonary artery pressure, right heart dilatation, right ventricle hypertrophy and reduced right ventricle ejection fraction were associated with procedural failure or success only with the use of an MRI-compatible guidewire. This result was somehow expected as catheter manipulation is more challenging in patients with dilated and dysfunctional heart chambers. The Authors also speculated that right heart chamber dilatation more than the high pulmonary artery pressure was

the reason for guidewire use or catheterization failure. Procedural time was not associated with tricuspid or pulmonary regurgitant fraction. So worsening disease was a predictor of more demanding and time-consuming procedures. All three unsuccessful cases underwent X-ray-guided right heart catheterization on the same day, two of them requiring a loop in the right atrium to reach the pulmonary arteries and one necessitated the use of a nitinol guidewire. X-Ray guidance was then explained because the looped shaft of a balloon wedge catheter cannot be visualised by CMR. The Authors could demonstrate the feasibility of MRI-guided catheterization even with adverse cardiopulmonary hemodynamics. Also in this experience procedures became significantly shorter with increasing operators' expertise and improved workflow. (38)

2.6 MRI-guided cardiac catheterization safety

There have been no described safety events related to CMR catheterization with minimal increase in patients' temperature during CMR. (34,36) Catheters can kink during MRI-guided catheterization, however, they can usually be removed by withdrawal uneventfully. (36)

The the safety profile of the procedure can be implemented by starting with adult patients and the gradually include older children by the time of getting enough expertise and be confident with the procedure. (34) Obviously, MRI-guided catheterization is not possible in patients who are not candidates for CMR due to the presence of metal in high risk locations (es intracranial implants) or previously implanted with pacemakers and defibrillators.

2.7 Indications for MRI-guided diagnostic cardiac catheterization

Several centers described their initial experience with MRI-guided cardiac catheterization, mainly for diagnostic purposes. Possible indications:

- Right and left heart catheterization
- Determine pulmonary vascular resistance and reactivity in pulmonary hypertension
- Cardiomyopathies
- Congenital heart disease and intracardiac shunts
- Univentricular heart palliated with Glenn or Fontan
- post-heart transplant surveillance

2.8 Interventional MRI-Guided cardiac procedures in humans

MRI is used in several cardiac units to guide endomyocardial biopsy and by electrophysiologists to guide electrophysiology studies and ablations. (12) Early experiences described aortic coarctation balloon angioplasty and pulmonary valvuloplasty in children and adults.

2.8.1 Endomyocardial biopsy

Endomyocardial biopsy is strongly recommended for new-onset heart failure associated with hemodynamic compromise or ventricular arrhythmias and is often performed for post-heart transplant surveillance (64) The diagnostic yield of endomyocardial biopsy varies and it depends on the disease distribution. (65) Fluoroscopy guided endomyocardial biopsy may cause false negative in focal disease processes which do not have a uniform distribution.

Rogers T, et al compared real-time MRI-guided to traditional fluoroscopy-guided endomyocardial biopsy in an animal model of focal myocardial pathology, demonstrating the improvement to guide targeted biopsy to the affected myocardium. Indeed, MRI guidance allowed to remarkable increase in the diagnostic yield of endomyocardial biopsy in comparison to X-Ray guided biopsy (82% versus 56% respectively, odds ratio: 1.43). (66) Real-time MRI-guided endomyocardial biopsy may reduce the number and size of specimens needed to have a more accurate diagnosis, decreasing the risk of complications such as tricuspid injury or myocardial perforation. Moreover, it may encourage left

ventricle biopsy when clinically indicated, due to the real-time visualisation of the bioptome and its interaction with the surrounding structures such as aortic and mitral valve. (66)

2.8.2 Electrophysiology studies and ablations

MRI-guided catheterization may be very useful in electrophysiology to navigate complex CHD patients, especially after multiple surgeries and interventions. Accurate visualisation of catheters and surrounding anatomical structures is essential for ablation, especially in single-ventricle physiology patients. Sommer P et al described the first series of five patients with real-time MRI-guided placement of multiple catheters with subsequent performance of stimulation maneuvers after ablation in a conventional EF laboratory. (67) MRI-guided cavotricuspid isthmus ablation was also demonstrated by the same group. (68) Finally, the feasibility and safety of CMR-based cryo-ablation system for cardiac ablation in a canine model have been demonstrated, allowing real-time catheter navigation, verification of catheter tip–tissue contact and intra-procedural assessment of ablations. (69,70)

2.8.3 Aortic coarctation balloon angioplasty

An early experience of MRI-guided cardiac interventions in humans was described in 2005 by the Deutsches Herzzentrum Berlin group in five patients with native or recurrent coarctation of the aorta who underwent balloon angioplasty. (71) Angioplasty balloon catheters (Tyshak II balloons) were filled with iron oxide–based contrast medium Resovist because CO2 could not be used due to the risk of gas embolism in case of balloon rupture. The patient's mean age was 18.9 ±12.2 years old. Two patients had a native contraction of the aorta, two had a previous balloon angioplasty and one had a surgical end-to-end anastomosis. The procedure was successful in four out of five patients with a significant reduction in the pressure gradient across the coarctation. In one patient the lesion was not responsive to dilatation. Volume-rendered 3D-MRI allowed accurate assessment of the aorta before and immediately after the procedure. (71)

2.8.4 Pulmonary valvuloplasty

Five years later the Evelina Children's Hospital group described two cases of pulmonary valvuloplasty in paediatric and adult patients. (49) They used MR-compatible valvuloplasty catheters (Tyshak II, NuMED, Hopkington, NY) in a 6-year-old boy with severe pulmonary valvar pulmonary and in a 43-year-old man

with valvar and subvalvar pulmonary stenosis. Real-time MRI showed complete waist abolition with improvement in the right ventricle to pulmonary artery gradient.

2.9 Interventional MRI-Guided cardiac procedures in animal models

2.9.1 Aortic coarctation stenting

Preclinical studies in swine demonstrated the safety and feasibility of real-time MRI-guided aortic coarctation stenting which allowed accurate procedure planning, device tracking, and stent implantation. This was confirmed immediately after the procedure with necropsy on 5 animals with showed correct stent implantation with no macroscopic evidence of heating injury or thrombus formation. Stents were implanted over active guidewire receiver coils, which significantly improved the visualisation in comparison to passive nitinol guidewires. Also the platinum and MP35N stents could be visualized as signal voids during real-time CMR. One unintentional and four intentional aortic ruptures were created during stent deployment due to an oversized balloon. The rupture was instantly visible under real-time MRI as an expanding extramural hematoma along the postero-lateral aorta. Then, CMR imaging could immediately identify complications such as aortic dissection or rupture, before angiographic confirmation or hemodynamic deterioration. (51) The advantage of this technique is that continuous stent and aortic wall visualisation can facilitate stent positioning and implantation with instantaneous haemodynamic confirmation of procedural success, providing also spatially resolved hemodynamic information. (72) This is particularly useful in complex coarctation where the superior tridimensional MRI anatomical information may smother the interventional procedure. Other advanced CMR tools may be used in future to immediately assess the procedural results such as aortic wall stiffness, distensibility, and compliance, which together with the clinical response may guide subsequent follow-up and management. (51)

2.9.2 Atrial septal defect closure

CMR-guided atrial septal defect (ASD) closure has been described in animals. ASD balloon sizing inflated with gadolinium under CMR was described in 14 pigs, obtaining identical measurements with MR and x-ray fluoroscopy. (73)

Different groups also performed atrial septal defect (ASD) and patent foramen ovale (PFO) closure in swine models under real-time MRI guidance with the use of Amplatzer septal occluder (ASO, AGA Medical Corporation, MN) or Self-made non-magnetic occluder. The perfect device to perform ASD device closure under real-time CMR should be metal-free and should be differentiated from myocardial tissue and blood at MRI. (74,75) Most groups used an Amplatzer Septal Occluder which is made of a nitinol wire mesh that produces low artefacts and good visualisation. These experiences demonstrated that CMR could accurately determine the ASD size before the intervention, and the procedural results also in terms of changes in right heart chamber volumes and function. (73,76,77) Rickers C et al, found a reduction right heart volumes soon after ASD closure (77) which corroborated the data of decreased right atrium area and right ventricle volumes by echocardiography within 24 hours after ASD closure. (78)
Device malposition during the wiggle manoeuvre was also demonstrated by real-time MRI, making feasible the occluder recapture and reposition. (76)

2.9.3 Ventricular septal defect closure

Real-time MRI-guided percutaneous muscular ventricular septal defect (VSD) closure was demonstrated in swine with direct transthoracic vascular access using a commercial nitinol device. (79)

2.9.4 Pericardiocentesis

CMR-guided pericardiocentesis was tested in swine using commercial 18G titanium puncture needles. The Authors suggest that continuous needle and pericardial effusion visualization of the needle allow easier puncture in challenging cases such as distorted thoracic anatomy or loculated effusion. (80)

2.9.5 Transeptal puncture of the fossa ovalis

Arepally A. et al also demonstrated the feasibility and safety of using a novel active MR transeptal needle system to perform transeptal puncture of the fossa ovalis in a swine with direct CMR visualization of a needle and the surrounding anatomical structures. (81)

2.9.6 Coronary catheterization

Zhang S et al performed a coronary catheterization in pigs with CMR guidance, underlying the limitation of MRI-guided catheterization for this application. Procedural time was unacceptably long ranging between 32 and 91 minutes mainly due to poor spatial resolution and single-projection imaging (41) However, another group performed successful real-time MR-guided coronary artery stent placement in a swine model with high-quality coronary images. There was a stent embolisation due to the wrong size choice, which was properly predicted during the procedure. (82)

2.10 Limitations of MRI-guided cardiac catheterization

Despite the enormous potential of MRI-guided cardiac catheterization interventions, its use in daily clinical practice is still limited. The main reason is the unavailability of MRI-compatible equipment, including wires, catheters, stents and devices. With commercially available balloon wedge catheters only the tip of the catheters could be visualised during real-time CMR and after some attempts catheters lost their stiffness in contact with blood.

Another possible reason is that in the early experiences, these procedures were performed in hybrid CMR/X-ray fluoroscopic suites often switching from one modality to the other. (38) This can be a potential issue to the broader adoption of this technique due to the high cost and challenging logistics. A dedicated interventional CMR workstations may offer live visualization of different planes, which may help in challenging cases.

However, many studies have demonstrated that is feasible and safe to perform MRI-guided catheterization with standard technology using an existent 1.5 T CMR scan, just having a preparation room for gaining access and for emergency evacuation in case of haemodynamic instability. (34,52)

Chapter 3

How to start an MRI-guided catheterization program

3.1 MRI-guided catheterization team

Different professionals are involved in the set-up and improvement of an MRI-guided cardiac catheterization program. The essential team is composed of an expert congenital interventional cardiologist, a paediatric cardiologist and/or radiologist with training in CMR imaging, a pediatric cardiac anaesthetist, catheterization laboratory nurses, MRI nurses and MRI technologists trained in real-time image guidance.
The team will need training in working and adapt in a new environment. In particular, the cath lab team should learn working in a different setting without X-ray and leads, while the MRI team will learn how to work in a sterile field, understanding the needs of the interventionalist. Many procedures are necessary to perfectly coordinate, developing protocols which allows real-time guidance of diagnostic and interventional procedures.

3.2 MRI-guided catheterization setting

Different settings are possible to start performing real-time MRI-guided procedures. In many centers, a biplane X-ray fluoroscopy room and an MRI room are nearby on the same floor to allow an easy transition from one room to another. In other centers the two rooms are adjacent or co-localized, just separated by radiofrequency shielded sliding doors allowing independent and combined use. In these rooms, interventional cardiologists can operate independently or together for MRI-guided procedures. This setting can be very expensive, precluding the possibility of building an MRI-guided catheterization suite in centers with limitations in space and funding. (83)

As an initial experience, is possible to get started with "MRI-augmented catheterization" with smooth transfer from the MRI room to the cath lab,

combining flow and shunt calculation by MRI followed by direct pressure measurement by fluoroscopy-guided cardiac catheterization. (39)

3.2.1 Preparation room

Having a room to be used for patient preparation is essential. This room should be as close as possible to the CMR and staffed with all the equipment, needed for patient preparation. In this room, anaesthesia induction is performed and the interventional cardiologist gains vascular access and prepares all the MRI-compatible equipment before entering the CMR room. Considering the age, clinical history and preferences of the patients mild sedation with intravenous benzodiazepines and local anaesthetic before venous sheath insertion was offered to patients as an alternative to general anaesthesia. Surface vector-cardiogram electrodes are attached, a phased array body coil is positioned and the sterile drape is folded over the patient. Vascular access is generally gained using ultrasound guidance to reduce the risk of vascular complications. [Figure 1 and 2] Femoral vein is the preferred approach, while jugular access is considered in case of blocked femoral veins. Suturing vascular access sheaths before transfer to the CMR can be considered to reduce the risk of accidental dislodgement, albeit this is unlikely because the patient lies on the same MRI-compatible detachable travelling table which is moved from the preparation room and then attached to the MRI scanner.
When the patient is ready to be transferred to the CMR a metal safety check is performed as all non-compatible equipment, should be removed from the magnetic field. Patient transfer from the preparation to CMR room should be performed in a straight line with no barriers, especially in patients with multiple lines, tubes and electrodes. (47)

This room should always be available and accessible when a MRI-guided procedure is performed to allow patient evacuation from the CMR scanner in case of haemodynamic instability and/or for pacing or defibrillation in case of unstable arrhythmia. Venous lines and tubes should exit the MRI scanner and be easily accessible in case of emergency evacuation. Longer lines and tubes are usually required with larger “dead space”. Unfortunately, MR-compatible defibrillators are not available. (84) Inotropic medication infusion or the need to test multiple hemodynamic conditions is generally possible during CMR catheterization. (34)

3.2.2 CMR room

In most centers, a 1.5T MRI scanner is needed to provide real-time images for catheters navigation. 3.0 T MRI scanners may offer a better signal in comparison

to 1.5 T, at the expense of increased device heating. CMR suite should contain MRI-conditional anaesthesia equipment, ventilators, infusion pumps and patient monitors, a hemodynamic recording system, two mirrored image displays (one in the control room and one in the CMR room) such as shielded projector systems or LCD monitors. The magnetic field can create ECG noise, which can be filtered by commercial equipment. (32) The introduction of new generation shorter and wider bore MRI scans has positively impacted the procedure, improving the operator's access to the patient. In-room image displays are available with RF shielding to be placed next to the magnet and in front of the interventionist. (39)
Usually, the MRI table is made sterile in the preparation room and then moved and attached to the MRI scanner. Moreover, the MRI scanner side is draped with sterile surgical drapes to avoid any contamination. [Figure 3] Planning is essential in regard to patient and monitors placement in the room, especially in terms of access to vascular lines and airway. A non-invasive blood pressure cuff and a peripheral oxygen saturation probe are attached to the patient for monitoring. MRI-compatible anaesthesia care equipment is generally available including MRI-compatible nitric oxide delivery systems, which can be used also for vasoreactivity testing in pulmonary arterial hypertension.

MRI scanners emit loud noise, therefore the interventional cardiologist performing the procedure should wear headsets paired with an MR-compatible microphone to protect against noise and communicate with the control room. [Figure 4] This is particularly import as this constant communication allows real-time guidance during procedures.

Chapter 4

MRI-guided catheterization procedure

4.1 Procedural planning

Planning the procedure is essential to optimise the procedural logistics and time. Sometimes, it is needed to gain alternative access as patients may have lost femoral access. In this case, particular attention should be paid to the procedural planning as an alternative to femoral access change also the logistic of the CMR room. For example, cases performed from the internal jugular vein may need repositioning of the hemodynamic recording system and in-room image display. The monitors should be placed to allow the interventional cardiologist to work from the groin and/or from the head. In most of the series, catheterization was performed via femoral access, even though many CMR rooms are equipped with displays both at the head and foot side. (34,36)

Usually, imaging planes are chosen before the procedure with clear communication between the interventional cardiologist and the MRI technologist. This helps shorten the procedural time, making it similar to the fluoroscopy-guided procedures, once teams get enough experience. (34,52)

4.2 Patient safety

Physicians, nurses and technologists should have a proper safety training. Special safety procedures are needed because MRI-guided catheterization is a unique procedure where ferromagnetic equipment is used in the preparation room and then the patient is moved to the MRI room. A "metal time-out" is mandatory before entering in the MRI room to ensure that non MRI-compatible materials become projectiles attracted by the MRI magnet.

4.3 Imaging equipment

1.5T MRI scanners are recommended for clinical MRI-guided catheterization as they provide a satisfactory temporal and spatial resolution. Indeed, these procedures need fast image acquisition, reconstruction and display to provide real-time images for procedural guidance. (38) MRI technologists develop protocols to modify image orientation and position interacting with the interventionist, to guarantee continuous visualisation of catheters and wires. CMR imaging localizers are generally obtained at abdominal and cardiac sites to allow catheter visualisation from the groin to the heart. (36) Interventional CMR computer systems have been developed and are available to simplify catheter real-time guidance. Many interventional cardiologists work under fluoroscopy at a frame rate between 4 and 15 frames/second, real-time CMR can easily offer images at 8-10 frames/second with better soft tissue visualisation but worse spatial resolution.

4.4 Cath equipment

One of the main challenges limiting the routine use of MRI-guided catheterization is the scarce availability of MRI-compatible and MRI-visible wires, catheters, sheaths and devices. Transducers, access sheaths and non-braided diagnostic catheters such as balloon wedge catheters are MRI-compatible. However, most of the catheters incorporate metal braiding for support, kink resistance and "torquability" and are attracted by the MRI magnet, acting as projectiles and susceptible to radiofrequency (RF) heating during the procedure, with potential harm for the patients and the operators. Indeed, due to the equipment's conductive properties, radiofrequency coupling can cause significant heating of the material. (85,86) Moreover, ferromagnetic equipment such as stainless steel coils or stents creates large artefacts, while nickel-titanium, platinum, gold, copper and plastic are less susceptible to artefacts. RF artefacts depend not only on magnetic field strength but also on the device size, orientation and imaging parameters. (39)

4.4.1 Catheters

In most centers, a single-lumen balloon wedge pressure catheter is used for right heart catheterizations. Polymer catheters are visualized exclusively by the contents of distal balloons filled with air, CO2 or dilute gadolinium contrast. Therefore, the catheter tip and shaft are always visible under fluoroscopy, whereas

only the tip is visible during MRI-guided catheterization, causing inferior visibility. This issue may limit catheter navigation, especially in congenital patients after surgical repair, dilated heart chambers or severe valvular regurgitation. (87) Gadolinium-filled balloons are usually seen more than air-filled balloons and can be selectively identified using a ‘saturation preparation’ CMR mode that enhances the appearance of gadolinium inside the wedge balloon. (36) Gadolinium-filled wedge catheters deflate satisfactorily though more slowly than air-filled balloons. Some Authors described simple modifications to metallic braided catheters which preserve the mechanical integrity while allowing CMR catheterization without RF-induced heating. (86)

4.4.2 Guidewires

During cardiac catheterization, guidewires aid the navigation in complex cardiovascular anatomies and their absence may result in increased procedure challenges and potential failure. Unfortunately, standard commercial metallic guidewires used for X-Ray-guided cardiac catheterization cannot be used under real-time CMR guidance. Metal is used for commercially available guidewires to ensure support and "torquability". (88) As seen for the catheters incorporating metal braiding, guidewire metals are responsible for RF heating and artefacts. Anyway, types of CE-marked 0.035″ CMR-conditional guidewires are available such as the Emery GlideTM MR Wire guidewire (Nano4Imaging, Germany) and the MRline guidewire (EPflex, Germany). The first is constructed from a high-strength core composite of glass fibers and polymers, protected by an aramid fiber mantle and covered with a PTFE extrusion. The EPflex MRline guidewire core is made of a high-strength polymeric material with an “MRI marker” of iron-platinum nanoparticles.

Several other guidewires have been described in vitro and in vivo in the last years. Some non-metallic polymer CMR-compatible guidewires with less stiffness and torque responsiveness are available with iron oxide tip for passive or active electronic visualization. (43,89) Glass-fiber-based guidewires made from micropultruded glass and/or aramid fibers and epoxy resin have been tested in vivo for evaluation of MR-guided endovascular interventions showing feasibility and safety in a swine model. These guidewires showed good to excellent visibility, with low artefacts and satisfactory stiffness and flexibility. (90)
Glass-fiber epoxy-based guidewire were also assessed by Li X et al during 3T MRI-guided cardiovascular catheterization in phantoms and porcine models. This group also confirmed the not significant heating of the guidewire, as the tip

heating did not exceed 0.35˚C when using low-SAR protocols with sufficient visualisation to support the catheterization procedure during real-time MRI. They could perform also left heart catheterization, successfully placing a braided curved AL2 catheter in the left ventricle in healthy swine using the glass-fiber epoxy-based guidewire under real-time MRI guidance. (91)

Self-made guidewires made of a resin-microparticle compound covered by polytetrafluoroethylene were successfully tested for MR-guided coronary artery catheterization in swine models (92) Despite feasible, as an average of 141 seconds were needed to cannulate coronaries from the carotid arteries, passive markers needed for real-time MR guidance obscured the anatomy of the small coronaries. (92,93) Brecher C et al, developed an MR-compatible guidewire made from fiber-reinforced plastics using a micro-pullwinding technology, with satisfactory bending, torsional and stiffness proprieties. (94)

Sonmez M et al designed a 0.035” active MRI-compatible guidewire with an internal fiberoptic temperature probe with satisfactory flexibility and entire length visibility. The presence of a distal solenoid attachment offered tip visibility and negligible heating, while real-time temperature monitoring could collect heating information without a negative effect on imaging. (43)

Campbell-Washburn AE et al hypothesized the safe use of standard commercial metallic guidewires by reducing the CMR low specific absorption rate (SAR). (95) This was possible by lessening excitation energy and prolonged readout times to reduce RF-induced heating and using a commercially available Terumo guidewire (0.035″ 150 cm angled-tip) because its nitinol core is completely insulated with expanded polytetrafluoroethylene (ePTFE). Parameters used in low-SAR setting generated a 67-fold reduction in heating compared to normal protocols. After in vitro and animal models, a Terumo guidewire using low SAR cardiovascular magnetic resonance was tested in seven patients with suspected pulmonary hypertension with no adverse events. Less than 0.1°C was generated by the Terumo Glidewire with low-SAR imaging during 2 minutes of continuous imaging. (87) In this experience, this specific guidewire could facilitate MRI-guided right heart catheterization, improving the visibility and stiffness of the shaft of a Swan-Ganz catheter. However, visualisation even in this setting remains inferior to X-Ray guided catheterization. (87)

4.5 MRI-guided catheterization step by step

Preliminary imaging is needed with conventional localizers as the first step before creating reference views from interactive real-time sequences, which will be then used for real-time catheter visualization. The most commonly used views for right heart catheterization are a bicaval view, the right ventricle long axis view and the pulmonary artery bifurcation view. (38) The catheter is advanced from the vascular access (femoral or jugular) through the inferior or superior vena cava, the right atrium, the right ventricle, pulmonary artery and wedge position under real-time CMR view. The MRI technologist selects the precise real-time planes and directly communicates with the interventionist to track the catheter by switching among the planned reference views. Pressure measurements are recorded in the right atrium, right ventricle, pulmonary artery and capillary wedge pressure. Mixed venous and pulmonary sample blood for oxygen saturation are obtained.

CMR flow analyses is performed in the proximal ascending aorta, sub-pulmonary artery and pulmonary artery branches using a conventional free breathing velocity-encoded phase contrast sequence in order to derive cardiac output. All CMR imaging and analysis are carried using commercially available sequences.

Chapter 5

Ospedale Pediatrico Bambino Gesù experience

1. Background

In recent years MRI-guided cardiac catheterization has emerged as a feasible and safe procedure, combining the benefit of cardiac catheterization with the advantages of CMR. (34,36) Real-time CMR guides catheter navigation through the heart chambers and vessels allowing simultaneous haemodynamic assessment, detailed tissue characterization and anatomical evaluation under the same sedation or anaesthesia conditions without the use of ionising radiation. (36,51,60)
Cardiac output, pulmonary artery pressure and pulmonary vascular resistance are crucial components of standard hemodynamic assessment. Usually, the Fick principle or thermodilution are used for these measurements, however, they are intrinsically inaccurate and imprecise as based on multiple measurements and assumptions. In contrast, velocity-encoded phase-contrast magnetic resonance is an established method to quantify blood flow and has been proven accurate. (56-58) However, the comparison of flows and pulmonary vascular resistances between the Fick principle and CMR flows had controversial results. We retrospectively report our initial experience of MRI-guided catheterization in children and patients with CHD, comparing the cardiac output and indexed pulmonary vascular resistance measured using the traditional Fick method and CMR flows under the same haemodynamic conditions.

2. Methods

Non-consecutive children and young adults affected by CHD or cardiomyopathy referred for cardiac catheterization and MRI between May 2022 and October 2024 were invited to undergo MRI-guided heart catheterization. All patients or their parents in case of <18 years old signed a written informed consent and completed an MR safety questionnaire. Exclusion criteria were ineligibility to perform CMR, cardiovascular instability, pregnancy or nursing and renal insufficiency defined by an estimated glomerular filtration rate < 30 mL/min/1.73m^2. Baseline demographics, clinical characteristics, procedural data, invasive hemodynamic findings, CMR flows and procedural complications were recorded. All MRI-guided catheterizations were performed in a suite equipped with a 1.5-Tesla MRI scanner (MAGNETOM Aera, Siemens Healthcare, Erlangen, Germany) adjacent to a preparation room at Ospedale Pediatrico Bambino Gesù in Rome. All procedures were performed by one of two paediatric interventional cardiologists with more than five years of experience in X-Ray guided catheterization. Two of the four paediatric interventional cardiologists involved in this procedure, one anesthesist and one CMR technologist from Ospedale Pediatrico Bambino Gesù spent a period of training with the cardiac magnetic resonance research group of the Royal Free London NHS Foundation Trust. During each procedure at least an interventional cardiologist, a radiologist, an anesthesist, a CMR technologist and a CMR nurse were present. Depending on the clinical scenario, the procedure was conducted either in an awake patient or under general anaesthesia. Vascular access to the femoral vein and artery was gained in the preparation room under ultrasound guidance. Alternative access such as the right internal jugular vein was considered in case of blocked femoral veins. Once access was gained and appropriate size short sheaths inserted, the MRI-compatible detachable travelling table was made sterile, cleared of any metallic equipment, moved to the CMR room and attached to the MRI scanner. Hemodynamic monitoring with 12-lead ECG, pulse oximetry sensors, non-invasive blood pressure and end-tidal CO2 was kept throughout the patient transfer. A CMR-compatible monitor was used to mirror the scanner display for in-room catheter visualization.

MRI-guided right heart catheterization was performed using an appropriate size 5F or 7F Corodyn™ wedge catheter (Braun Interventional Systems Inc., Pennsylvania, United States) monitoring wedge pressure balloon flotation catheter with single pressure lumen filled with air, which produced a signal void on imaging. [Figure 5] An MRI conditional wire Emery Glide Straight Cp MR Wire (Nano4Imaging GmbH, Aachen, Germany) was used when the catheter alone could not reach the desired chamber or vessel. The catheters were navigated

through the heart and vessels under real-time MRI guidance. Procedural success was defined as the completion of a full right heart catheterization. Pressure measurements and traces were recorded in the right atrium, right ventricle, pulmonary arteries and pulmonary wedge. Systemic, mixed and pulmonary sample blood for oxygen saturation were obtained at the same haemodynamic and sedation conditions. Haemodynamic data and pulmonary vascular resistance were assessed under 25% fraction of inspired oxygen (FiO2).

Systemic blood flow (Qp) and pulmonary blood flow (Qs) were obtained by phase contrast CMR and compared to the Fick principle. LaFarge-Miettinen formula was used to estimate oxygen consumption (VO2) and utilised for cardiac output calculations with the Fick principle. (53) CMR flow analyses was performed in the proximal ascending aorta, sub-pulmonary artery and pulmonary artery branches using a conventional free breathing velocity-encoded phase contrast sequence.

The total pulmonary blood flow to total systemic blood flow, the Qp/Qs ratio was used to quantify the net shunt.

Pulmonary vascular resistance (PVR) was calculated as:
PVR = (mean pulmonary artery pressure– mean pulmonary wedge pressure)/Qp.

Indexed PVR (PVRi) was calculated as:
PVRi = PVR / BSA.

2.1 Imaging settings

Initial imaging included localizer sequences and the acquisition of dedicated planes optimized for interventional catheter navigation. CMR catheterization was performed using an interactive real-time balanced steady-state free precession (bSSFP) sequence, employing up to three interleaved imaging planes oriented along different axes to enhance catheter visualization. Subsequently, anatomical reference planes of the right atrium, right ventricle, and pulmonary arteries were obtained to facilitate catheter navigation through the right heart, ultimately advancing into the pulmonary arteries and reaching the wedge position. Following catheter navigation, phase-contrast (PC) flow imaging was performed at the level of the proximal ascending aorta, main pulmonary artery, and branch pulmonary arteries. Velocity encoding (VENC) values were individualized for each patient. Cardiac volumes and function were evaluated using breath-hold SSFP cine imaging. Breath-holds were manually coordinated by the anesthesiologist. Additional imaging, such as cine long-axis (LAX) views, 3D

morphological sequences, or late gadolinium enhancement (LGE) were acquired as needed to complete the diagnostic evaluation.

2.2 Statistical analysis

Data were analyzed with SPSS v22.0. (International Business Machines, Chicago, IL) Continuous variables are presented as mean ± standard deviation, while categorical variables as percentages. Linear regression was used to compare cardiac index, pulmonary index, Qp:Qs and PVRi. A p-value of <0.05 was considered significant. Flow measurement techniques, Qp:Qs and PVRi were compared using Bland-Altman analysis. The differences between the 2 methods were expressed as mean difference and mean percentage difference.

3. Results

3.1 Baseline demographic and clinical details

Twenty-five patients, thirteen males and twelve females, were invited to undergo MRI-guided heart catheterization. All of them accepted to participate in the study and signed the informed consent. Cardiac catheterization and CMR were clinically indicated in all patients. The study population was composed of paediatric or young adult patients with complex CHD or cardiomyopathy. The mean age was 12.3 ± 11.1 years old and the mean weight was 35.7 ± 22.5 Kg with a mean BSA of 1.1 ± 0.5 m^2. Most of the patients had a cardiomyopathy and the indication for catheterization was surveillance and/or placement on the heart transplant list (n = 13; 52%; nine restrictive cardiomyopathy, two hypertrophic cardiomyopathy, one dilated cardiomyopathy and one chronic inflammatory cardiomyopathy). Seven patients were univentricular heart palliated with Glenn (n = 2) and Fontan (n = 5), tricuspid valve anomalies (n =1), total anomalous pulmonary venous return post-repair (n =1), double outlet right ventricle post-repair (n =1), Uhl's anomaly (n =1) and congenitally corrected transposition of great arteries palliated with pulmonary artery banding (n =1).

3.2 Procedural success and timings

A complete MRI-guided cardiac catheterization was performed successfully in 96% of patients. In one case the pulmonary arteries could not be reached due to severely dilated right atrium and right ventricle in an adolescent with a Uhl's anomaly. This patient was transferred to the cath lab and pulmonary arteries could be reached with the use of a hydrophilic 0.035" Terumo wire (Terumo Corporation, Tokyo, Japan) under X-ray guidance. For the other patients right heart catheterization was not repeated under X-ray guidance.

Most of the procedures were performed from a femoral access (n = 23; 92%). In the two patients palliated with a Glenn a right internal jugular access was also gained to access the pulmonary arteries. In the other two patients (one patient with restrictive cardiomyopathy and one with congenitally corrected transposition of great arteries palliated with pulmonary artery banding) femoral access could not be gained so right heart catheterization was performed from the right internal jugular vein. Intravenous heparin (100 IU/kg) was administered, aiming for an activated clotting time (ACT) target >200 s. In most of the patients, the MRI-guided catheterization was performed under general anaesthesia with mechanical ventilation (n=20; 80%). The remaining 5 patients were awake and only local anaesthesia was given. Procedural time ranged between 120 and 280 minutes

including catheterization and CMR imaging. Procedures became significantly shorter with increasing procedural experience using standard real-time CMR imaging planes.

3.3 Patient safety

Radiation-free MRI-guided catheterization was performed in all subjects with no cases of bailout to X-Ray, except for one patient. There were no procedural complications related to MRI-guided catheterization and no patient experienced hemodynamic instability or needed resuscitation. There were no cases of early termination of CMR catheterization due to technical equipment or CMR issues. Metal safety check was performed in all cases preventing ferromagnetic equipment presence in the MRI room in all procedures. After the procedure, two patients reported access site bruising which was managed conservatively.

3.4 Hemodynamic assessment

MRI-guided cardiac catheterization haemodynamic findings are described in [Table 1]. The Cardiac index measurements with the Fick method were slightly higher in comparison to MRI flows (3.15 ± 0.82 L/min/m^2 and 3.00 ± 0.95 L/min/m^2 respectively). There was a moderate correlation between cardiac index measurement techniques (R^2 0.59; p< .001). The Bland-Altman Analysis showed a mean difference of 0.15 ± 0.61 L/min/m2, 95% CI -1.04 to 1.34 L/min/m2, which corresponded to a mean percentage difference of 6.1 ± 20.1%. [Figure 6]

The pulmonary index measurements with the Fick method were slightly higher in comparison to MRI flows (2.97 ± 0.73 L/min/m^2 and 2.67 ± 0.72 L/min/m^2 respectively). There was a moderate correlation between pulmonary index measurement techniques (R^2 0.42; p< .001). The Bland-Altman Analysis showed a mean difference of 0.29 ± 0.61 L/min/m2, 95% CI -0.90 to 1.49 L/min/m2, which corresponded to a mean percentage difference of 11.1 ± 21.9%. [Figure 7]

The QP:Qs measurements with the Fick method were similar in comparison to MRI flows (0.95 ± 0.12 and 0.92 ± 0.17 respectively). There was a significant correlation between QP:Qs measurement techniques (R^2 0.83; p< .001). The Bland-Altman Analysis showed a mean difference of 0.03 ± 0.07, 95% CI -0.12 to 0.18, which corresponded to a mean percentage difference of 4.1 ± 11.5%. [Figure 8]

The indexed pulmonary vascular resistance measurements with the Fick method were slightly lower in comparison to MRI flows (2.33 ± 1.35 WU*m^2 and 2.57 ± 1.26 WU*m^2 respectively). There was a strong correlation between PVRi techniques (R^2 0.86; $p < .001$). The Bland-Altman Analysis showed a mean difference of -0.23 ± 0.51 WU*m^2, 95% CI -1.23 to 0.76 WU*m^2, which corresponded to a mean percentage difference of -11.2 ± 23.0%. [Figure 9]

4. Discussion

4.1 Feasibility of MRI-guided catheterization

In this study, we report Ospedale Pediatrico Bambino Gesù experience with radiation-free MRI-guided cardiac catheterization in children and patients with CHD. We used previously described passive tracking sequences in a heterogeneous population of patients with cardiomyopathies, complex CHD and post-surgical anatomies, referred for diagnostic cardiac catheterization and pulmonary vascular resistance assessment. We could obtain invasive and CMR data under the same haemodynamic conditions with reasonable agreement between flow measurements and PVRi with the Fick method and the phase-contrast–derived MRI flows.

After the first description in 2003 by Razavi R et al, many centers worldwide have started MRI-guided catheterization programs with good results. Previous studies have described different CMR settings and software, catheters and guidewires, passive and active tracking. Patients with cardiomyopathies or complex CHD usually require multiple diagnostic and interventional catheterization during their life, being exposed to ionising radiation with possible radiation-induced chromosomal damage, increasing the risk of developing cancer. (29)

Cardiomyopathy assessment was the main indication for MRI-guided catheterization in our series. This was an excellent starting point to get experience in a "normal" biventricular heart, acquiring the necessary experience to manipulate catheters under real-time CMR in more challenging anatomies. Overall, the success rate was 96% without the need for bailout fluoroscopy. There was only one failure to access the pulmonary arteries without a guidewire in a 29 Kg Uhl's anomaly patient with severely dilated right heart chambers. This is in line with reports from Rogers T and Ratnayaka K group who failed to reach the pulmonary artery with a balloon wedge pressure catheter in a few patients with severely dilated right atrium and ventricle caused by pulmonary hypertension. (36,52) In these selected cases, when difficulties can be anticipated, a catheterization laboratory should be available and free to complete the haemodynamic assessment under fluoroscopy guidance often with the help of a hydrophilic guidewire. In all cases, the procedure was performed using a 5F or 7F balloon wedge catheter filled with air. The 5F wedge catheters which were used in smaller children lack support, kink resistance and "torquability", especially after a few minutes of manipulation inside the vessels. Moreover, only the tip of this

catheter is visible limiting catheter navigation, especially in small children and CHD patients after surgical repair.

As already reported by other Authors, MRI-guided catheterization is also feasible in patients with single ventricle anatomy status post Glenn or Fontan. (35,63,96) In our series, the procedure could be performed in all seven patients with a Glenn or Fontan physiology without a bailout X-Ray procedure. This special population needs non-femoral access (Glenn) to enter the pulmonary arteries and often a guidewire is necessary to cross the conduit fenestration (Fontan) to assess atrial and ventricular pressures when indicated. Imaging planes oriented along different axes are similar and catheters course is even straighter than the right ventricle to pulmonary artery trajectory. The feasibility of this procedure in this population is extremely important because these are the patients most exposed to multiple catheterizations, thus reducing the risk of DNA damage and developing cancer during follow-up. (29)

Despite the advancement of MRI-guided catheterization, some technical challenges need to be addressed to expand a broader adoption of this method. One of the most encountered issues in real-time CMR guidance is the continuous need for manual updating of the imaging plane to track the balloon wedge catheter tip during navigation. This was particularly true in patients with severe right heart chamber dilatation, slowing the procedures because of continuous relocation of the catheter tip. This limitation is also the reason for procedural failure or the necessity to use a guidewire as demonstrated by Knight DS et al. (38). Interestingly, with the actual technology the average balloon visibility is less than 70% of the scanning time (63) However, some Authors demonstrated that balloon wedge catheter visibility can be improved to around 90% of the procedure by acquiring a heavily T1-weighted image with a large slice thickness and overlaying this onto a high-resolution image of the selected anatomical structure. (97,98) Neofytou AP et al developed an automatic, deep-learning post-processing pipeline for automatic tracking of the catheter and imaging plane during MRI-guided catheterization. The images are dynamically acquired on three contiguous slices, and the planes are automatically adjusted when the catheter falls in one of the outer slices. This approach was assessed in seven patients showing high accuracy specificity and sensitivity of this tracking strategy with compatibility with real-time conditions. (98)

4.2 Safety of MRI-guided catheterization

Procedures were performed safely in all patients without any adverse events. Team training and communication were essential to increase the safety of this procedure. (99) Many professionals were involved and they needed to adapt to a new environment, working together. Proper communication included clear information flow and a reciprocal comprehensive understanding of various needs. The interventional cardiologists should anticipate their preferred imaging planes before the beginning of the procedure and mutual feedback and reciprocal knowledge usually improve the team results. Proper training for sterile field maintenance was adopted among the team, especially for professionals not used to working in the catheterization laboratory. Developing protocols may reduce risks and improve procedural performance.

To reduce risks we decided to start with older children weighing more than 30 Kg in order to gain confidence with the new procedure and get enough expertise to perform more complex procedures. In our series, we confirmed the very low risk of RF-induced catheter heating if proper catheters are used. (34,36). One catheter was kinked during the procedure in a child with restrictive cardiomyopathy but could be easily removed, as described in other experiences. Despite the impossibility of seeing the catheter shaft the catheter kink was recognized based on change in tactile feedback. (36)

We also performed a "metal time-out" in the preparation room before entering the MRI room. The first operator and the nurse cleared the sterile field and all the ferromagnetic equipment was counted to ensure that non-MRI-compatible materials became projectiles attracted by the MRI magnet. To further reduce the risk of introducing metals in the MRI scan we always open the same number of syringes and puncture needles, leaving on the sterile field only catheters, an MRI-compatible wire, two syringes for flushing, four syringes for blood gases and a plastic bowl with saline. Subsequently, one anesthesiologist, two CMR nurses and a CMR technologist performed patient transfer to the MRI scan. This process was facilitated by the use of an MRI-compatible detachable travelling table where patients lay during all procedural time. Patient safety was also guaranteed by continuous patient monitoring and high-fidelity haemodynamic and ECG recording.

Urgent evacuation from the CMR scan was not needed in our series and none of the patients needed urgent resuscitation manoeuvres. However, we planned

evacuation strategies with prompt evacuation to the preparation room in case of emergency such as haemodynamic instability and/or ventricular arrhythmia.

4.3 Radiation sparing

The main advantage of MRI-guided catheterization is combining haemodynamic assessment and detailed tissue characterization and anatomical evaluation without the use of ionising radiation. In our series, this technique allowed avoiding X-Ray exposure and the hazards associated with ionising radiation in 24 out of 25 patients. Despite the increased attention to radiation exposure with subsequent accurate radiation dose optimisation in children over the years, the risk for children often requiring multiple long procedures remains important. Ait-Ali L et al tried to determine the lifetime risk of developing cancer associated with radiation exposure in 59 children with complex CHD. They found that the lifetime attributable risk to develop cancer for a 1-year-old child was 1 in 382 for male and 1 in 156 for female patients. Moreover, there was a statistically significant increase in micronucleus assay as a biomarker of DNA damage and long-term risk predictor of cancer 2 hours after catheterization procedures in comparison with baseline assessment. (29) Growing children are more radiosensitive than adults and live longer to experience the hazard of radiation toxicity.

Most of the patients in our series had more than one previous catheterization during their life. This is particularly true in the two most represented populations of this preliminary experience: children with cardiomyopathies and patients with single ventricle physiology palliated with Glenn or Fontan procedures. (100-103) Moreover, especially patients with univentricular heart require long procedure and prolonged X-ray exposure, which may include interventions on the Fontan conduit, Fontan fenestration, pulmonary arteries, veno-venous collaterals, aortic arch etc.

4.4 Comparison between Fick and Phase-Contrast MR

Our series demonstrates a reasonable agreement between flow measurements and PVRi with the Fick method and the phase-contrast–derived MRI flows. This result confirms the data previously obtained in other experiences. Already in 2004, Muthurangu V et al demonstrated a good correlation between the two methods in children and adults with suspected PH or CHD. (28) The data was then corroborated in children post-heart transplant, simple shunts, pulmonary

hypertension, cardiomyopathy, valvular and heart disease (34) and in 102 patients with and without pulmonary hypertension. (52)

Controversial is the agreement between the two methods during the vasoreactivity test with inhaled nitric oxide and oxygen. Indeed Rogers T et al reported a stronger correlation on the vasoreactivity test than Muthurangu et al (28), speculating that this result could be explained by the higher number of paired calculations, use of estimated VO2 and lower mean PVRi at baseline. (52)

However, it is known that the Fick principle is not precise in patients with large intracardiac shunt and high pulmonary blood flow due to reduced pulmonary arteriovenous oxygen content difference. This can explain why pulmonary vasodilation test with high-concentration oxygen further reduces the accuracy of this principle as the oxygen content of pulmonary artery become similar to the oxygen content of aortic blood at baseline.

On the contrary, Muthurangu et al could demonstrate on phantom studies the accuracy of phase-contrast MR even at high flow rates. (28,57) They concluded that the worse agreement between the Fick method and the phase-contrast–derived MRI flows after pulmonary vasodilation tests may be caused by errors in the Fick. (28) In our series flow measurements were slightly higher with the Fick method in comparison to MRI flows. Also, this result matches with the experience of Ratnayaka et in children with mixed conditions ranging from pulmonary hypertension to simple shunts and cardiomyopathies. (34)

5. Future direction

MRI-guided catheterization has evolved in the last decade to clinical routine in several centers. Though availability of MRI-compatible and MRI-visible equipment remains the main problem for the widespread implementation of this procedure, some efforts have been made by industry to address this issue.

However, current research efforts are now shifting more to imaging systems than catheterization equipment, with the goal reduce RF heating of metal-made catheters and devices under CMR. (47) Some groups described the use of low-specific absorption rate (SAR) imaging protocol which can reduce the amount of radio energy applied to create the images reducing significantly equipment heating. (87) Other groups proposed lower field MRI, for example modifying a 1.5T scanner to operate at 0.55T, to reduce existing catheterization equipment heating, maintaining adequate image quality. The concept is that at lower magnetic fields, the RF which is needed to create images is reduced as the metal equipment heating. (47,104) The routine introduction of low-field imaging may increase the use of available catheterization equipment and reduce artefacts.

There is potential for MR-guided catheterization to grow, finding its role also in interventional cardiology. This procedure may significantly improve the management of patients with complex CHD, providing instant assessment of the outcome of an intervention and guiding additional treatment and follow-up. It may help the development and optimization of new procedures and assist alternative access such as transthoracic access to the heart due to visualization of the whole thorax. (79,105)

Rogers T et al described successful percutaneous transthoracic left atrium access directly from the posterior chest wall under real-time MRI guidance. This kind of percutaneous approach to the left atrium was described in the 1950s using long needles through the posterior chest wall. (106) It needs iatrogenic lung deflation, which is generally associated with low morbidity and mortality. (107) This alternative access to the left atrium has the potential to offer a more direct and coaxial route for transcatheter mitral valve interventions. In this experience, the left atrium access was closed with an off-the-shelf atrial septal occluder (105)

Percutaneous cavo-pulmonary anastomosis and shunt creation were successfully demonstrated in fifteen swine using an MRI antenna needle to create a pathway between the superior vena cava and the pulmonary artery bifurcation under real-time MRI guidance. Overlapping pre-mounted covered CP stents or a purpose-

built self-expanding device were then implanted. (96) MRI guidance was crucial in this successful preliminary experience as it allowed transmural puncture of two contiguous vessels avoiding surrounding critical structures such as the aorta. The target vessel (main pulmonary artery–right pulmonary junction) was always visualised, making the needle trajectory even more accurate. This experience was translated in humans the following year with the first-in-human fully percutaneous bidirectional Glenn operation under fluoroscopy in a 35-year-old woman with a functional single ventricle and restrictive pulmonary blood flow. (108,109)

The substantial advantage of MRI-guided catheterization in the field of interventional cardiology is the possibility to assess the real-time interaction of used devices and the surrounding anatomical structures and tissues. For example, results of stent or device implantation can be assessed instantaneously, as the possible complications such as vessel dissection, rupture or pericardial effusion. (37) Moreover, in the future would be possible the integration of MRI-guided catheterization with pressure-volume loop assessment, which can add interesting information on myocardial functional analysis. Kuehne T et al determined right ventricle myocardial contractility from MRI-derived pressure-volume loops in patients with pulmonary hypertension demonstrating that pressure overload was associated with reduced right ventricle function. (110)

Finally, some groups hypothesised promising implementation of exercise MRI-guided catheterization as a clinical tool to unmask subtle conditions. Patients with unexplained dyspnea, chest pain and normal testing at rest may benefit most from this tool. (52). In 2016 the Great Ormond Street Hospital group demonstrated the feasibility and safety of MR-augmented cardiopulmonary exercise testing in healthy and CHD children. Exercise tests were performed on an MR-compatible ergometer, oxygen uptake was continuously acquired and simultaneous cardiac output was measured using a real-time MR flow sequence. They demonstrated abnormal exercise patterns in oxygen uptake, cardiac output, and arteriovenous oxygen content difference in patients with pulmonary hypertension and repaired Tetralogy of Fallot. (111)

6. Limitations

This preliminary experience carries some limitations being a retrospective study with a relatively small sample. Moreover, we did not enroll consecutive patients, making the study population highly heterogeneous with difficult comparison of the different subgroups. Indeed, we started with adults and older children (>30 Kg) to get enough experience to safely perform MRI-guided catheterization in smaller patients and be more inclusive.

The scarcity of MRI-compatible catheterization equipment and CMR time slots limited the routine adoption of MRI-guided catheterization in our center. We used commercially available balloon wedge catheters filled with air, however, only the tip of the catheters could be visualised during real-time CMR and after some attempts catheters lost their stiffness in contact with blood. We performed MRI-guided catheterization with standard technology using our existent 1.5 T CMR scan, however, a dedicated interventional CMR workstation may offer live visualization of different planes, which may help in challenging cases.

Finally, we routinely performed MRI-guided catheterization via the femoral approach apart in the patients palliated with a Glenn and when femoral veins were no more accessible after multiple procedures. However, in some cases, the internal jugular venous approach could have been even advantageous with potentially reduced catheter manipulation which could have been a benefit in this setting.

7. Conclusions

MRI-guided catheterization is feasible and safe in children and patients with CHD and can be performed with standard technology using existent CMR scans. MRI combines a better soft tissue visualisation with additional haemodynamic information obtained by catheterization, without the use of X-Ray, reducing the risks associated with ionising radiation. A full anatomical, functional and haemodynamic assessment can be obtained during the same anaesthesia and under the same conditions. Flow measurements and pulmonary vascular resistance obtained by CMR and with the traditional Fick method have a good correlation at the baseline condition. Training and effective communication between team members involved in this procedure is essential. Advancements in MRI technology with improved image quality, faster scanning times, and dedicated catheterization equipment may increase the role of MRI-guided catheterization in CHD and open more space for interventional procedures. Sharing experience, knowledge and innovation and building consensus among the CHD international community is needed for a true clinical translation of these preliminary experiences.

Chapter 6

Interesting cases

6.1 Uhl's anomaly

A 10-year-old, 29 kg child from Marocco was referred to our unit for worsened exercise tolerance and persistent vomiting. The parents were cousins but there was no family history of CHD or sudden death during childhood. The child suffered recurrent respiratory infections and reduced exercise tolerance in the past. At the age of 8, the parents consulted a healthcare provider in Morocco who diagnosed severe tricuspid regurgitation and prescribed oral diuretics, potassium and iron. A few months after moving to Italy, she came to our emergency department with worsening symptoms of right heart failure.

After a routine diagnostic work-up, we decided to perform an MRI-guided cardiac catheterization in general anaesthesia. The CMR demonstrated extreme dilation of the right ventricle (RVEDVi 618 ml/m2, RVEDV/LVEDV ratio of approximately 16), with severe global systolic dysfunction (RVEF 13%), with poor/absent representation of the ventricular myocardium. Severely dilated tricuspid annulus with free tricuspid regurgitation (RF approximately 80%) with marked dilation of the right atrium, inferior vena cava and suprahepatic veins. There was diffuse linear enhancement of the walls of the right ventricle, with a thin LGE extending also to the right side of the interventricular septum. The size of the left ventricle was normal (LVEDVi 37 ml/m2) with mild-moderate systolic dysfunction (LVEF 40%). Marked interventricular septum dyskinesia with inversion of the septal curvature in the diastolic phase.
The pulmonary arteries were free from discrete stenosis, with angulation of the left pulmonary artery at the origin, compressed posteriorly by the severe cardiomegaly, and referential flow to the right pulmonary artery (RPA/LPA = 76%/24%). These findings were compatible with the clinical suspicion of Uhl's anomaly with severe impairment of right ventricular function. The cardiac index measured by CMR flows was 2.1 L/min/m2. [Figure 10]

The catheterization was performed under real-time MRI guidance. Through the right femoral vein, a 7F Corodyn™ wedge catheter (Braun Interventional Systems

Inc., Pennsylvania, United States) filled with air was easily advanced to the right atrium and right ventricle. Even with the use of an MRI conditional wire Emery Glide Straight Cp MR Wire (Nano4Imaging GmbH, Aachen, Germany), it was not possible to reach the pulmonary arteries. The haemodynamic data, confirmed at the subsequent X-Ray guided catheterization to assess pulmonary artery pressure and wedge pressure, showed an equalization of the right sections pressures (RA -/-/21 mmHg, RV 31/15/23 mmHg, PAs 29/17/22 mmHg, wedge pressure -/-/15). Systemic saturation was 97%, mixed venous and pulmonary artery saturations were 55%. So the Cardiac index by Fick was 2.4 L/min/m2 with PVRi of 2.9 WU.m2.

The patient was listed for a heart transplant and discharged. She was re-admitted a few weeks later for episodes of vomiting and abdominal pain. She was deteriorating on inotropic support and was finally transplanted. She suffered acute rejection on the third day post-transplant, which was successfully treated with ev steroids, thymoglobulins, eculizumab and alemtuzumab. She was finally discharged home, continuing her cardiological follow-up.

6.2 Fontan circulation

A 30-year-old woman with tricuspid atresia, normally correlated great vessels and pulmonary stenosis was referred to our unit. She was palliated in another center with a modified right Blalock-Taussing shunt followed by a Glenn procedure and finally with a Fontan procedure with a 20 mm extra-cardiac fenestrated conduit. In the last months, she was experiencing reduced exercise tolerance, which was confirmed by a cardiopulmonary test. We decided to electively perform an MRI-guided catheterization to assess the Fontan anatomy, function and haemodynamics. The entire procedure was performed with the patient awake and local anaesthetic.

CMR showed a significant narrowing at the mid portion of the Fontan conduit with concentric wall thickening, probably calcified, and associated flow acceleration. There were no significant pulmonary artery branches stenosis with balanced flow distribution. The left ventricle was of normal size and function (LVEDVi 59 ml/m2, LVEF 64%). The liver was enlarged, with irregular margins and diffuse inhomogeneous parenchyma. [Figure 11a]

Hemodynamyc data confirmed the conduit stenosis with a pressure gradient of 2 mmHg (-/-/12 mmHg below the stenosis and -/-/10 mmHg above it). There was good agreement between Cardiac index and indexed pulmonary vascular resistance between Fick method and CMR flows (CI by Fick 2,8 L/min/m^2 vs CI by CMR 2,6 L/min/m^2, PVRi by Fick 1,8 WU.m^2 vs PVRi by CMR 1,9 WU.m^2).

In view of this data we discussed the case with the case manager of the patient and decided to proceed one month later with stenting of her Fontan conduit.
The procedure was performed under X-Ray guidance and general anaesthesia. Angiography in the Fontan conduit confirmed the stenosis at the level of the middle tract of the conduit, measuring approximately 10 mm. Direct stenting of the Fontan conduit was performed with a 22x48 mm BeGraft Bentley covered stent (Bentley InnoMed GmbH, Germany) which was post-dilated with a 20x40 mm Atlas Gold PTA balloon (Bard Medical). There was almost complete abolition of the waist (minimum diameter in the central portion around 17 mm) and complete abolition of the gradient. [Figure 11b]

There were no procedural complications and the patient was discharged the following day, doing well during follow-up. Anticoagulation was prescribed for three months after the procedure, followed by aspirin only long-life. The subsequent cardiopulmonary test demonstrated an improvement in functional

capacity with a peak VO2 of 22.4 ml/kg/min equal to 60% according to normative values proposed by Wasserman equation and between the 75th and 90th percentile of the values detected in similar populations in comparison to a peak VO2 of 19.6 ml/kg/min before the stenting procedure.

Chapter 7

Research activity undertaken throughout the PhD programme

7.1 Description of the specific issues tackled in the research activity

The research activity tackled several critical topics in paediatric cardiology, especially in the field of interventional cardiology. The specific issues addressed included:

• *New devices in CHD*. Atrial flow regulator implantation in patients with CHD and children with severe pulmonary hypertension or cardiomyopathy, demonstrating the promising and beneficial effects in this population in the short-term follow-up.

• *Implantable hemodynamic monitors in CHD*. Feasibility and safety of percutaneous implantation of the CardioMEMS device in a selected population of adults and children with CHD. The potential of this device in reducing HF hospitalization in this setting is enormous, with uncertainty on the adherence to the regular transmission of hemodynamic data in the congenital population.

• 4D Flow magnetic resonance in Tetralogy of Fallot (ToF). Describe by means of 4D flow MRI and computational fluid dynamics simulations the hemodynamics of operated ToF patients with transannular patches undergoing routine follow-up MRI before percutaneous or surgical pulmonary valve implantation and its possible association with clinical outcomes.

• Management and percutaneous treatment of pulmonary vein stenosis.

• Use of Pressure-volume loops in CHD.

• Transcatheter palliation with pulmonary artery flow restrictors in neonates with CHD.

• Bedside transcatheter patent ductus arteriosus device closure in premature neonates.

• Education in CHD community. Coordination and evaluation of the role of e-learning postgraduate education in collaboration with the Association for European Paediatric and Congenital Cardiology.

7.2 List of the main publications

1. Piccinelli E, Heying R, Albert-Brotons DC, Bosschers L, Milanesi O, Voges I, Sendzikaite S, Pitkänen-Argillander O, Michel-Behnke I, McMahon CJ. Enhancing paediatric and congenital cardiology e-learning postgraduate education: insights from the Association for European Paediatric and Congenital Cardiology directed webinar series. Cardiol Young. 2025 Feb;35(2):388-392. doi: 10.1017/S1047951124036448.

2. Piccinelli E, Grutter G, Pilati M, Rebonato M, Scalera ST, Adorisio R, Amodeo A, Ingrasciotta G, Mencarelli E, Galletti L, Butera G. Use of the CardioMEMS Device in Children and Patients with Congenital Heart Disease: A Literature Review. J. Clin.Med. 2024, 13(14):4234. https://doi.org/10.3390/jcm13144234.

3. Montefoschi D, Pilati M, Fausti E, Pina M, Martinelli M, Di Marco P, Rebonato M, Piccinelli E, Scalera S, Perfili M, Cannata V and Butera G. The Importance of Weight-Based Protocols and Reduction of Frame Rates in ASD Percutaneous Closure. Clin Radiol Imaging J. 2024, 8(1): 000222.

4. Piccinelli E, Frazzetto F, Pilati M, Butera G. Stent Implantation Across the Atrial Flow Regulator Device. Pediatr Cardiol. 2024 Mar;45(3):695-698. doi: 10.1007/s00246-024-03405-z.

5. Butera G, Piccinelli E, Kolesnik A, Averin K, Seaman C, Castaldi B, Cuppini E, Fraisse A, Bautista-Rodriguez C, Hascoet S, D'Amore C, Baruteau A, Betrian Blasco P, Bianco L, Eicken A, Jones M, Kuo JA, Rajszys GB. Implantation of atrial flow regulator devices in patients with congenital heart disease and children with severe pulmonary hypertension or cardiomyopathy - an international multicenter case series. Front Cardiovasc Med. 2024 Jan 15;10:1332395. doi: 10.3389/fcvm.2023.1332395.

6. Piccinelli E, Butera G. Surgical repair of peripheral pulmonary artery stenosis: Is there still a place for transcatheter interventions? J Thorac Cardiovasc Surg. 2024 Apr;167(4):e98. doi: 10.1016/j.jtcvs.2023.10.032.

7. Hascoët S, Bentham JR, Giugno L, Betrián-Blasco P, Kempny A, Houeijeh A, Baho H, Sharma SR, Jones MI, Biernacka EK, Combes N, Georgiev S, Bouvaist H, Martins JD, Kantzis M, Turner M, Schubert S, Jalal Z, Butera G,

Malekzadeh-Milani S, Valdeolmillos E, Karsenty C, Ödemiş E, Aldebert P, Haas NA, Khatib I, Wåhlander H, Gaio G, Mendoza A, Arif S, Castaldi B, Dohlen G, Carere RG, Del Cerro-Marin MJ, Kitzmüller E, Hermuzi A, Carminati M, Guérin P, Tengler A, Fraisse A, EUROPULMS3 investigators. Outcomes of transcatheter pulmonary SAPIEN 3 valve implantation: an international registry. Eur Heart J. 2023 Oct 24:ehad663. doi: 10.1093/eurheartj/ehad663.

8. Piccinelli E, Testa A, Butera G. Versatility of Atrial Flow Regulator Device in Congenital Heart Disease: A Case Series. Pediatr Cardiol. 2023 Feb 16. doi: 10.1007/s00246-023-03123-y.

Figures

Figure 1. Preparation room. The patient lies on the same MRI-compatible detachable traveling table which is then moved to the MRI scanner. Anaesthesia induction and mechanical ventilation is performed. Surface vector-cardiogram electrodes are attached, a phased array body coil positioned and groins are prepared with antiseptic solution.

Figure 2. Preparation room. The sterile drape is folded over the patient. Vascular access is gained using ultrasound guidance and catheterization equipment is prepared. A metal safety check is performed before moving the patient to the magnetic field.

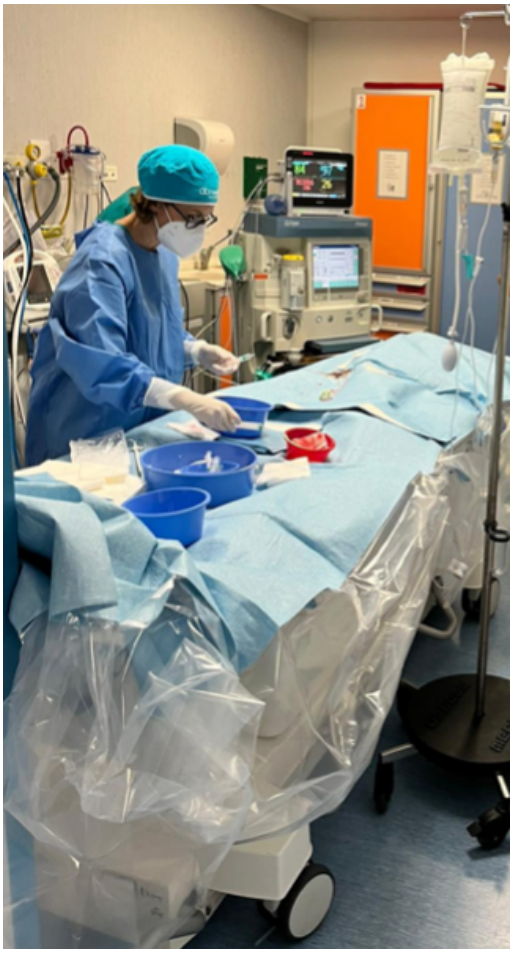

Figure 3. CMR room. The MRI-compatible detachable table is moved to the MRI scanner. The MRI scanner side is draped with sterile surgical drapes to avoid any contamination. Our CMR suite contains MRI-conditional anaesthesia equipment, ventilators, infusion pumps and patient monitors, haemodynamic recording system, and a CMR-compatible monitor to mirror the scanner display for in-room catheter visualization.

Figure 4. MRI scanner control room. A radiologist and an MRI technologist interact with the interventionists during the procedure, to guarantee MRI continuous visualisation of catheters and wires. Two mirrored images displays allow simultaneous visualisation in the control room and in the CMR room.

Figure 5. The tip of a Corodyn™ balloon wedge catheter filled with air is visualised in the main pulmonary artery as a signal void on CMR imaging (white arrow).

Figure 6. a. A moderate correlation between cardiac index calculated with the Fick principle and with CMR flow at baseline (R2 0.59; p< .001). b. Bland-Altman plot of the two flow measurement methods.

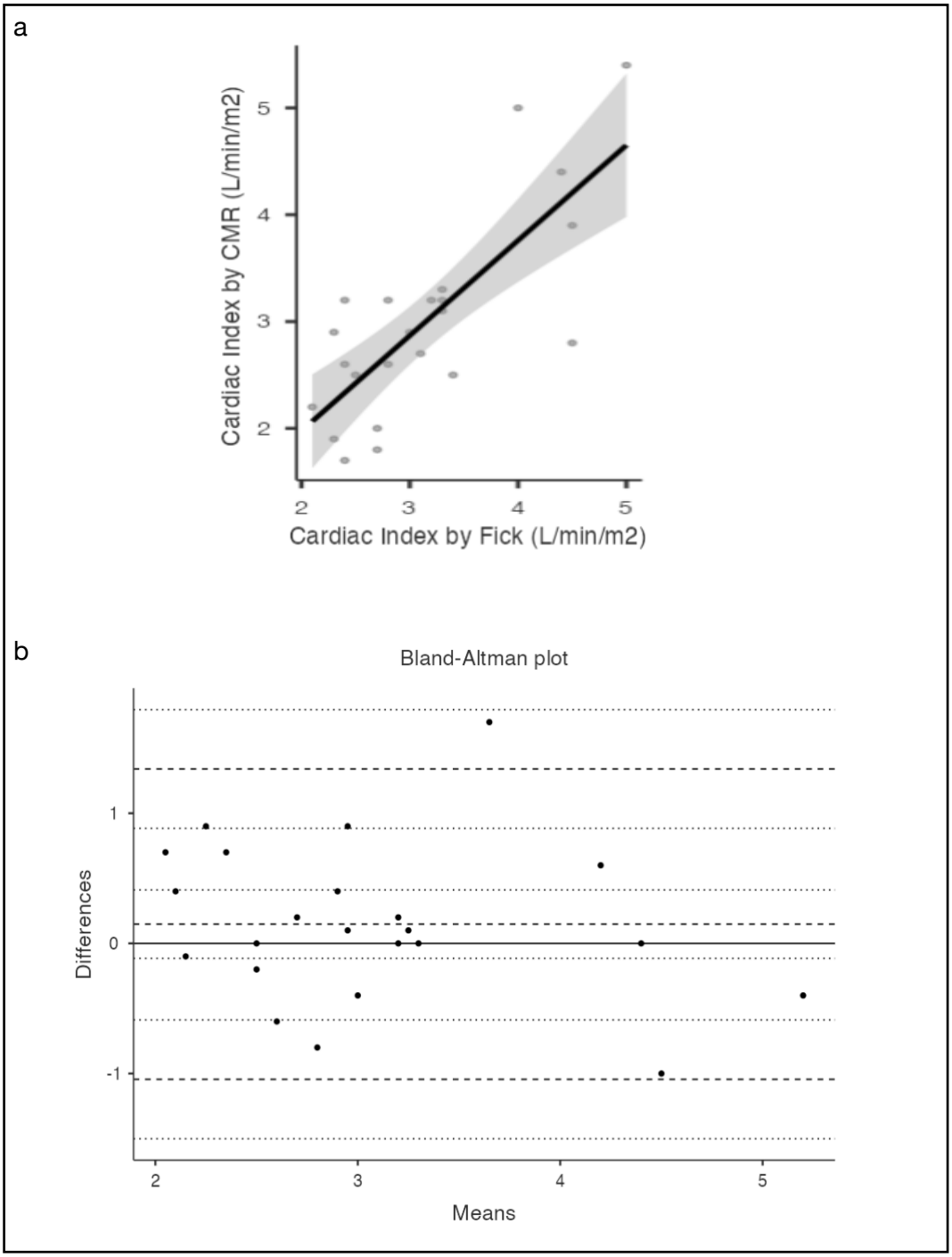

Figure 7. a. A moderate correlation between pulmonary index calculated with the Fick principle and with CMR flow at baseline (R^2 0.42; $p < .001$). b. Bland-Altman plot of the two flow measurement methods.

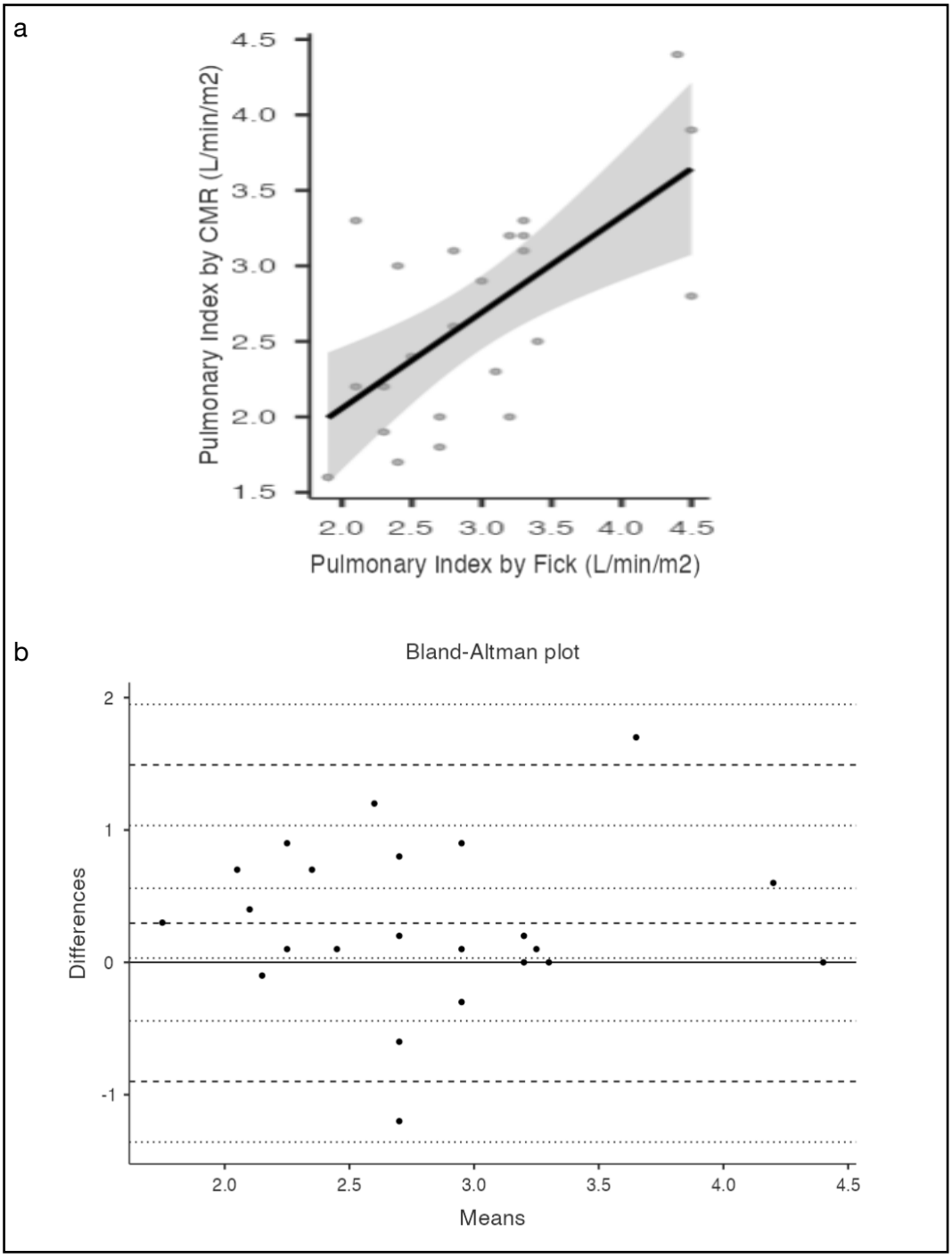

Figure 8. a. A significant correlation between Qp:Qs calculated with the Fick principle and with CMR flow at baseline (R^2 0.83; $p < .001$). b. Bland-Altman plot of Qp:Qs with the two measurement methods.

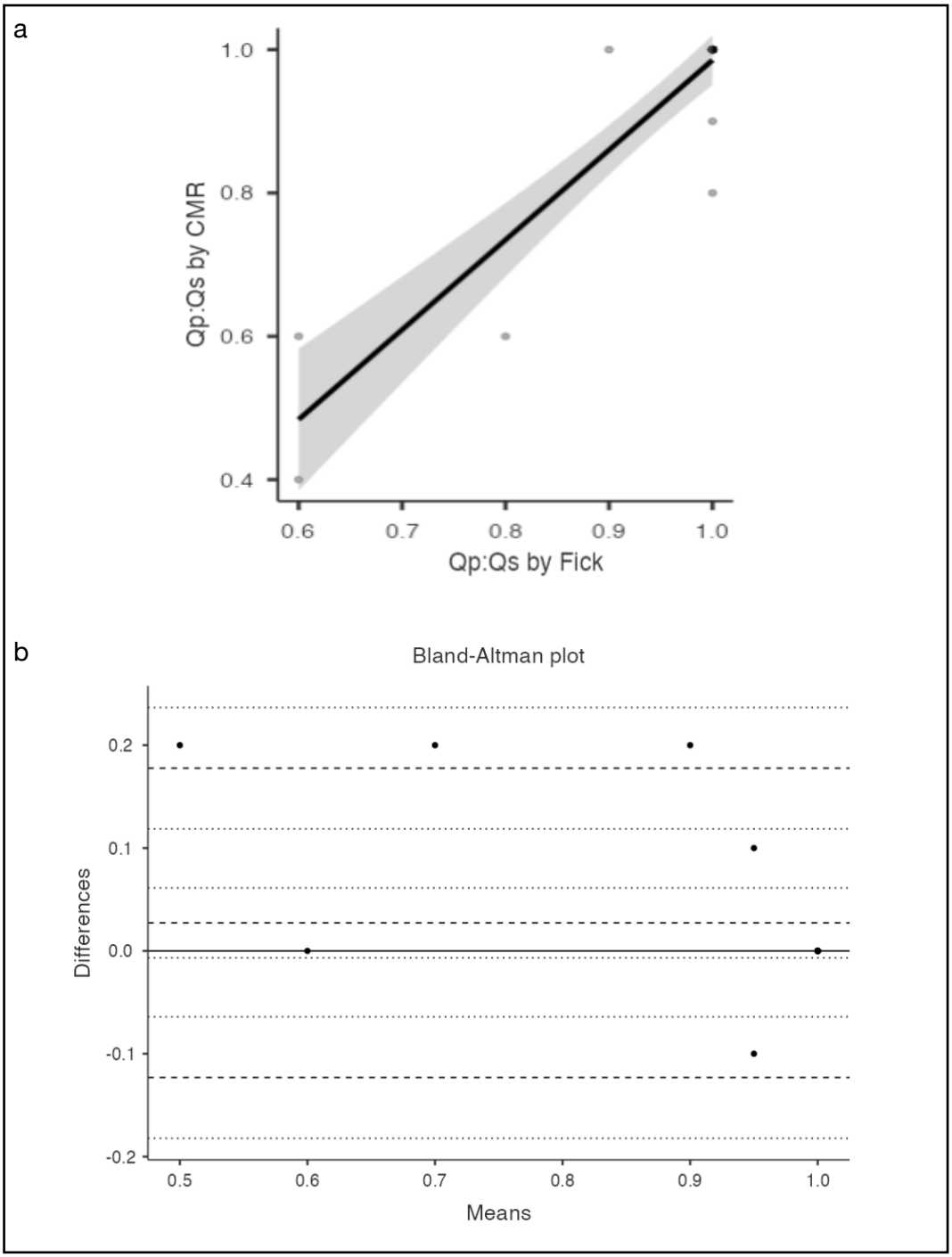

Figure 9. a. A significant correlation between indexed pulmonary vascular resistance (PVRi) calculated with the Fick principle and with CMR flow at baseline (R^2 0.86; p< .001). b. Bland-Altman plot of PVRi with the two measurement methods.

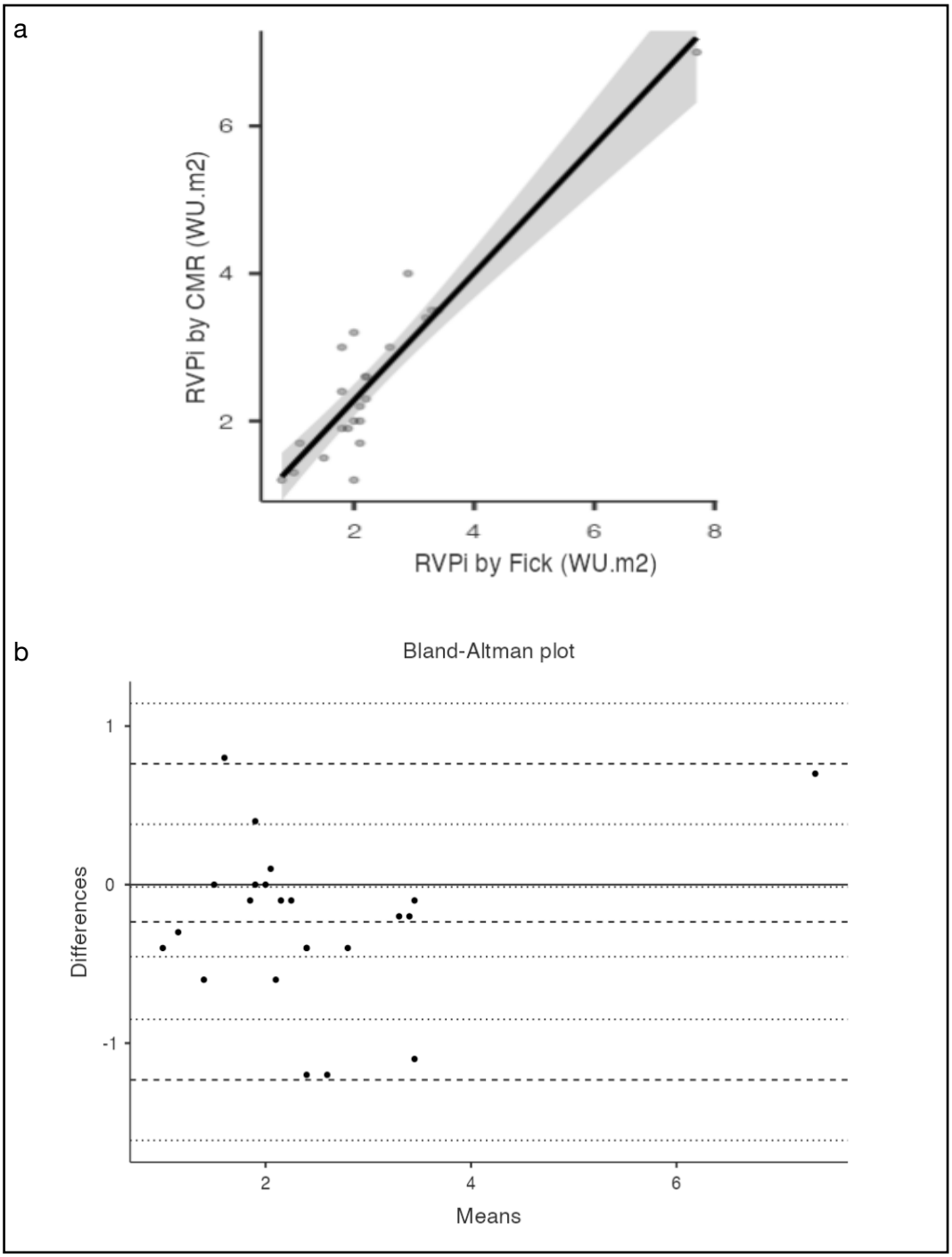

Figure 10. Uhl's anomaly on CMR with extreme dilation of the right ventricle (RVEDVi 618 ml/m2), poor/absent representation of the ventricular myocardium and marked interventricular septum dyskinesia with inversion of the septal curvature in the diastolic phase.

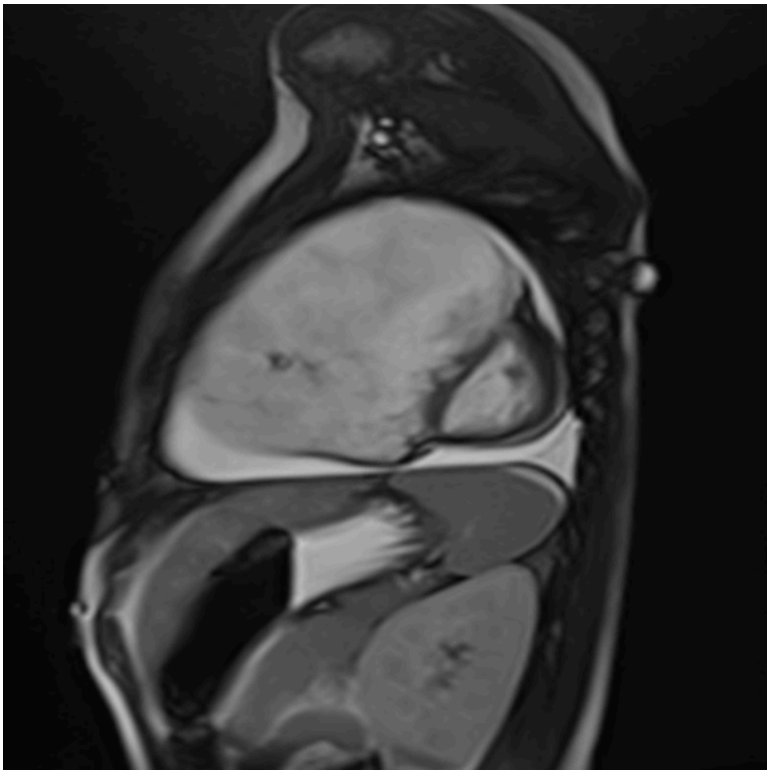

Figure 11. a. CMR shows a significant narrowing at the mid portion of the Fontan conduit with concentric calcified wall thickening. b. Direct stenting of the Fontan conduit with a 22x48 mm BeGraft Bentley covered stent, post-dilated with a 20x40 mm Atlas balloon.

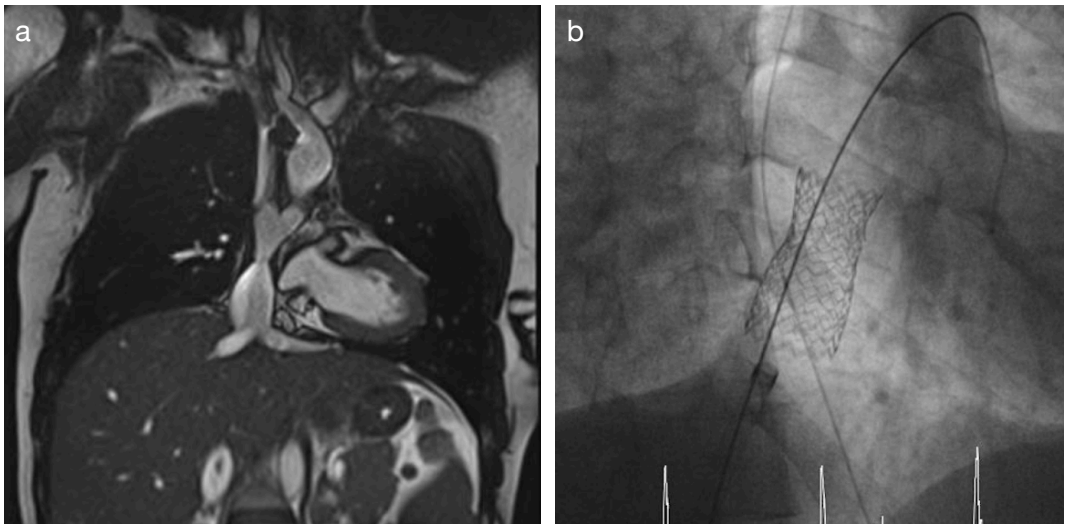

Table

Table 1. MRI-guided cardiac catheterization haemodynamic findings. Mean pulmonary artery pressure (mPAP), mean aortic pressure (mAo), right atrium (RA), right ventricle (RV), pulmonary wedge pressure (PWP), transpulmonary gradient (TPG), cardiac index (CI), pulmonary index (PI), indexed pulmonary vascular resistance (PVRi).

	Baseline (n=25)
mPAP (mmHg)	20.9 ± 8.3
mAo (mmHg)	68.9 ± 15.1
RA (mmHg)	9.7 ± 3.7
PWP (mmHg)	14.1 ± 6.2
TPG (mmHg)	6.8 ± 3.5
Systemic sat (%)	97.6 ± 2.9
Mixed venous sat (%)	70.5 ± 10.7
Pulmonary artery sat (%)	72.6 ±4.5
CI Fick (L/min/m^2)	3.2 ±0.8
PI Fick (L/min/m^2)	3.0 ± 0.7
QP: QS Fick	1.0 ± 0.1
PVRi Fick (WU*m^2)	2.3 ± 1.4
CI CMR (L/min/m^2)	3.0 ± 0.9
PI CMR (L/min/m^2)	2.7 ± 0.7
QP: QS CMR	0.9 ± 0.2
PVRi CMR (WU*m^2)	2.6 ±1.3

Bibliography

1. van der Linde D, Konings EE, Slager MA, Witsenburg M, Helbing WA, Takkenberg JJ, Roos-Hesselink JW. Birth prevalence of congenital heart disease worldwide: a systematic review and meta-analysis. J Am Coll Cardiol 2011;58(21):2241-7.

2. Liu Y, Chen S, Zuhlke L, Black GC, Choy MK, Li N, Keavney BD. Global birth prevalence of congenital heart defects 1970-2017: updated systematic review and meta-analysis of 260 studies. Int J Epidemiol 2019;48(2):455-463.

3. Baumgartner H, De Backer J, Babu-Narayan SV, Budts W, Chessa M, Diller GP, Lung B, Kluin J, Lang IM, Meijboom F and others. 2020 ESC Guidelines for the management of adult congenital heart disease. Eur Heart J 2021;42(6):563-645.

4. Saad H, Casey F, Dolk H, Loane M. Prevalence and trends of congenital heart defects among live births from 2005 to 2014 in Northern Ireland. Cardiol Young 2023;33(6):939-945.

5. Marelli AJ, Ionescu-Ittu R, Mackie AS, Guo L, Dendukuri N, Kaouache M. Lifetime prevalence of congenital heart disease in the general population from 2000 to 2010. Circulation 2014;130(9):749-56.

6. Geva T, Vick GW, 3rd, Wendt RE, Rokey R. Role of spin echo and cine magnetic resonance imaging in presurgical planning of heterotaxy syndrome. Comparison with echocardiography and catheterization. Circulation 1994;90(1):348-56.

7. Gaydos SS, Varga-Szemes A, Judd RN, Suranyi P, Gregg D. Imaging in Adult Congenital Heart Disease. Journal of Thoracic Imaging 2017;32(4):205-216.

8. Rizk J. 4D flow MRI applications in congenital heart disease. European Radiology 2021;31(2):1160-1174.

9. Di Salvo G, Miller O, Babu Narayan S, Li W, Budts W, Valsangiacomo Buechel ER, Frigiola A, van den Bosch AE, Bonello B, Mertens L and others. Imaging the adult with congenital heart disease: a multimodality imaging

approach-position paper from the EACVI. Eur Heart J Cardiovasc Imaging 2018;19(10):1077-1098.

10. Alsunbuli A. The use of cardiac magnetic resonance imaging (CMRI) for adult congenital heart disease patients: qualitative comparative review. Clin Med (Lond) 2020;20(Suppl 2):s6-s7.

11. Humbert M, Kovacs G, Hoeper MM, Badagliacca R, Berger RMF, Brida M, Carlsen J, Coats AJS, Escribano-Subias P, Ferrari P and others. 2022 ESC/ERS Guidelines for the diagnosis and treatment of pulmonary hypertension. Eur Heart J 2022;43(38):3618-3731.

12. Amin EK, Campbell-Washburn A, Ratnayaka K. MRI-Guided Cardiac Catheterization in Congenital Heart Disease: How to Get Started. Curr Cardiol Rep 2022;24(4):419-429.

13. Kolte D, Lakshmanan S, Jankowich MD, Brittain EL, Maron BA, Choudhary G. Mild Pulmonary Hypertension Is Associated With Increased Mortality: A Systematic Review and Meta-Analysis. J Am Heart Assoc 2018;7(18):e009729.

14. Simonneau G, Montani D, Celermajer DS, Denton CP, Gatzoulis MA, Krowka M, Williams PG, Souza R. Haemodynamic definitions and updated clinical classification of pulmonary hypertension. Eur Respir J 2019;53(1).

15. Leber L, Beaudet A, Muller A. Epidemiology of pulmonary arterial hypertension and chronic thromboembolic pulmonary hypertension: identification of the most accurate estimates from a systematic literature review. Pulm Circ 2021;11(1):2045894020977300.

16. Nagavci B, Tonia T, Roche N, Genton C, Vaccaro V, Humbert M, Brightling C, Robalo Cordeiro C, Bush A. European Respiratory Society clinical practice guidelines: methodological guidance. ERJ Open Res 2022;8(1).

17. Paulus WJ, Tschope C, Sanderson JE, Rusconi C, Flachskampf FA, Rademakers FE, Marino P, Smiseth OA, De Keulenaer G, Leite-Moreira AF and others. How to diagnose diastolic heart failure: a consensus statement on the diagnosis of heart failure with normal left ventricular ejection fraction by the Heart Failure and Echocardiography Associations of the European Society of Cardiology. Eur Heart J 2007;28(20):2539-50.

18. Kovacs G, Berghold A, Scheidl S, Olschewski H. Pulmonary arterial pressure during rest and exercise in healthy subjects: a systematic review. Eur Respir J 2009;34(4):888-94.

19. Maron BA, Brittain EL, Hess E, Waldo SW, Baron AE, Huang S, Goldstein RH, Assad T, Wertheim BM, Alba GA and others. Pulmonary vascular resistance and clinical outcomes in patients with pulmonary hypertension: a retrospective cohort study. Lancet Respir Med 2020;8(9):873-884.

20. Engelfriet PM, Duffels MG, Moller T, Boersma E, Tijssen JG, Thaulow E, Gatzoulis MA, Mulder BJ. Pulmonary arterial hypertension in adults born with a heart septal defect: the Euro Heart Survey on adult congenital heart disease. Heart 2007;93(6):682-7.

21. Manes A, Palazzini M, Leci E, Bacchi Reggiani ML, Branzi A, Galie N. Current era survival of patients with pulmonary arterial hypertension associated with congenital heart disease: a comparison between clinical subgroups. Eur Heart J 2014;35(11):716-24.

22. van Riel AC, Schuuring MJ, van Hessen ID, Zwinderman AH, Cozijnsen L, Reichert CL, Hoorntje JC, Wagenaar LJ, Post MC, van Dijk AP and others. Contemporary prevalence of pulmonary arterial hypertension in adult congenital heart disease following the updated clinical classification. Int J Cardiol 2014;174(2):299-305.

23. Ntiloudi D, Zanos S, Gatzoulis MA, Karvounis H, Giannakoulas G. How to evaluate patients with congenital heart disease-related pulmonary arterial hypertension. Expert Rev Cardiovasc Ther 2019;17(1):11-18.

24. Lammers AE, Bauer LJ, Diller GP, Helm PC, Abdul-Khaliq H, Bauer UMM, Baumgartner H, German Competence Network for Congenital Heart Defects I. Pulmonary hypertension after shunt closure in patients with simple congenital heart defects. Int J Cardiol 2020;308:28-32.

25. Diller GP, Kempny A, Alonso-Gonzalez R, Swan L, Uebing A, Li W, Babu-Narayan S, Wort SJ, Dimopoulos K, Gatzoulis MA. Survival Prospects and Circumstances of Death in Contemporary Adult Congenital Heart Disease Patients Under Follow-Up at a Large Tertiary Centre. Circulation 2015;132(22):2118-25.

26. Regitz-Zagrosek V, Roos-Hesselink JW, Bauersachs J, Blomstrom-Lundqvist C, Cifkova R, De Bonis M, Iung B, Johnson MR, Kintscher U, Kranke P and others. 2018 ESC Guidelines for the management of cardiovascular diseases during pregnancy. Kardiol Pol 2019;77(3):245-326.

27. Dhingra VK, Fenwick JC, Walley KR, Chittock DR, Ronco JJ. Lack of agreement between thermodilution and fick cardiac output in critically ill patients. Chest 2002;122(3):990-7.

28. Muthurangu V, Taylor A, Andriantsimiavona R, Hegde S, Miquel ME, Tulloh R, Baker E, Hill DL, Razavi RS. Novel method of quantifying pulmonary vascular resistance by use of simultaneous invasive pressure monitoring and phase-contrast magnetic resonance flow. Circulation 2004;110(7):826-34.

29. Ait-Ali L, Andreassi MG, Foffa I, Spadoni I, Vano E, Picano E. Cumulative patient effective dose and acute radiation-induced chromosomal DNA damage in children with congenital heart disease. Heart 2010;96(4):269-74.

30. Andreassi MG, Ait-Ali L, Botto N, Manfredi S, Mottola G, Picano E. Cardiac catheterization and long-term chromosomal damage in children with congenital heart disease. Eur Heart J 2006;27(22):2703-8.

31. Kleinerman RA. Cancer risks following diagnostic and therapeutic radiation exposure in children. Pediatr Radiol 2006;36 Suppl 2(Suppl 2):121-5.

32. Ratnayaka K, Faranesh AZ, Guttman MA, Kocaturk O, Saikus CE, Lederman RJ. Interventional cardiovascular magnetic resonance: still tantalizing. J Cardiovasc Magn Reson 2008;10(1):62.

33. Johnson JN, Hornik CP, Li JS, Benjamin DK, Jr., Yoshizumi TT, Reiman RE, Frush DP, Hill KD. Cumulative radiation exposure and cancer risk estimation in children with heart disease. Circulation 2014;130(2):161-7.

34. Ratnayaka K, Kanter JP, Faranesh AZ, Grant EK, Olivieri LJ, Cross RR, Cronin IF, Hamann KS, Campbell-Washburn AE, O'Brien KJ and others. Radiation-free CMR diagnostic heart catheterization in children. J Cardiovasc Magn Reson 2017;19(1):65.

35. Razavi R, Hill DL, Keevil SF, Miquel ME, Muthurangu V, Hegde S, Rhode K, Barnett M, van Vaals J, Hawkes DJ and others. Cardiac catheterisation

guided by MRI in children and adults with congenital heart disease. Lancet 2003;362(9399):1877-82.

36. Ratnayaka K, Faranesh AZ, Hansen MS, Stine AM, Halabi M, Barbash IM, Schenke WH, Wright VJ, Grant LP, Kellman P and others. Real-time MRI-guided right heart catheterization in adults using passive catheters. Eur Heart J 2013;34(5):380-9.

37. Rogers T, Ratnayaka K, Lederman RJ. MRI catheterization in cardiopulmonary disease. Chest 2014;145(1):30-36.

38. Knight DS, Kotecha T, Martinez-Naharro A, Brown JT, Bertelli M, Fontana M, Muthurangu V, Coghlan JG. Cardiovascular magnetic resonance-guided right heart catheterization in a conventional CMR environment - predictors of procedure success and duration in pulmonary artery hypertension. J Cardiovasc Magn Reson 2019;21(1):57.

39. Moore P. MRI-guided congenital cardiac catheterization and intervention: the future? Catheter Cardiovasc Interv 2005;66(1):1-8.

40. Settecase F, Martin AJ, Lillaney P, Losey A, Hetts SW. Magnetic Resonance-Guided Passive Catheter Tracking for Endovascular Therapy. Magn Reson Imaging Clin N Am 2015;23(4):591-605.

41. Zhang S, Rafie S, Chen Y, Hillenbrand CM, Wacker FK, Duerk JL, Lewin JS. In vivo cardiovascular catheterization under real-time MRI guidance. J Magn Reson Imaging 2006;24(4):914-7.

42. Kocaturk O, Kim AH, Saikus CE, Guttman MA, Faranesh AZ, Ozturk C, Lederman RJ. Active two-channel 0.035" guidewire for interventional cardiovascular MRI. J Magn Reson Imaging 2009;30(2):461-5.

43. Sonmez M, Saikus CE, Bell JA, Franson DN, Halabi M, Faranesh AZ, Ozturk C, Lederman RJ, Kocaturk O. MRI active guidewire with an embedded temperature probe and providing a distinct tip signal to enhance clinical safety. J Cardiovasc Magn Reson 2012;14(1):38.

44. Wang W. Magnetic Resonance-guided Active Catheter Tracking. Magn Reson Imaging Clin N Am 2015;23(4):579-89.

45. Hilbert S, Sommer P, Gutberlet M, Gaspar T, Foldyna B, Piorkowski C, Weiss S, Lloyd T, Schnackenburg B, Krueger S and others. Real-time magnetic resonance-guided ablation of typical right atrial flutter using a combination of active catheter tracking and passive catheter visualization in man: initial results from a consecutive patient series. Europace 2016;18(4):572-7.

46. Alipour A, Meyer ES, Dumoulin CL, Watkins RD, Elahi H, Loew W, Schweitzer J, Olson G, Chen Y, Tao S and others. MRI Conditional Actively Tracked Metallic Electrophysiology Catheters and Guidewires With Miniature Tethered Radio-Frequency Traps: Theory, Design, and Validation. IEEE Trans Biomed Eng 2020;67(6):1616-1627.

47. Nageotte SJ, Lederman RJ, Ratnayaka K. MRI Catheterization: Ready for Broad Adoption. Pediatr Cardiol 2020;41(3):503-513.

48. Guttman MA, Ozturk C, Raval AN, Raman VK, Dick AJ, DeSilva R, Karmarkar P, Lederman RJ, McVeigh ER. Interventional cardiovascular procedures guided by real-time MR imaging: an interactive interface using multiple slices, adaptive projection modes and live 3D renderings. J Magn Reson Imaging 2007;26(6):1429-35.

49. Tzifa A, Krombach GA, Kramer N, Kruger S, Schutte A, von Walter M, Schaeffter T, Qureshi S, Krasemann T, Rosenthal E and others. Magnetic resonance-guided cardiac interventions using magnetic resonance-compatible devices: a preclinical study and first-in-man congenital interventions. Circ Cardiovasc Interv 2010;3(6):585-92.

50. Abuzeid W, Abunassar J, Leis JA, Tang V, Wong B, Ko DT, Wijeysundera HC. Radiation safety in the cardiac catheterization lab: A time series quality improvement initiative. Cardiovasc Revasc Med 2017;18(5S1):S22-S26.

51. Raval AN, Telep JD, Guttman MA, Ozturk C, Jones M, Thompson RB, Wright VJ, Schenke WH, DeSilva R, Aviles RJ and others. Real-time magnetic resonance imaging-guided stenting of aortic coarctation with commercially available catheter devices in Swine. Circulation 2005;112(5):699-706.

52. Rogers T, Ratnayaka K, Khan JM, Stine A, Schenke WH, Grant LP, Mazal JR, Grant EK, Campbell-Washburn A, Hansen MS and others. CMR fluoroscopy right heart catheterization for cardiac output and pulmonary vascular resistance: results in 102 patients. J Cardiovasc Magn Reson 2017;19(1):54.

53. Lafarge CG, Miettinen OS. The estimation of oxygen consumption. Cardiovascular Research 1970;4(1):23-30.

54. Hillis LD, Firth BG, Winniford MD. Analysis of factors affecting the variability of Fick versus indicator dilution measurements of cardiac output. Am J Cardiol 1985;56(12):764-8.

55. Cigarroa RG, Lange RA, Hillis LD. Oximetric quantitation of intracardiac left-to-right shunting: limitations of the Qp/Qs ratio. Am J Cardiol 1989;64(3):246-7.

56. Hundley WG, Li HF, Hillis LD, Meshack BM, Lange RA, Willard JE, Landau C, Peshock RM. Quantitation of cardiac output with velocity-encoded, phase-difference magnetic resonance imaging. Am J Cardiol 1995;75(17):1250-5.

57. Beerbaum P, Korperich H, Barth P, Esdorn H, Gieseke J, Meyer H. Noninvasive quantification of left-to-right shunt in pediatric patients: phase-contrast cine magnetic resonance imaging compared with invasive oximetry. Circulation 2001;103(20):2476-82.

58. Robertson MB, Kohler U, Hoskins PR, Marshall I. Quantitative analysis of PC MRI velocity maps: pulsatile flow in cylindrical vessels. Magn Reson Imaging 2001;19(5):685-95.

59. Schalla S, Saeed M, Higgins CB, Martin A, Weber O, Moore P. Magnetic resonance--guided cardiac catheterization in a swine model of atrial septal defect. Circulation 2003;108(15):1865-70.

60. Muthurangu V, Atkinson D, Sermesant M, Miquel ME, Hegde S, Johnson R, Andriantsimiavona R, Taylor AM, Baker E, Tulloh R and others. Measurement of total pulmonary arterial compliance using invasive pressure monitoring and MR flow quantification during MR-guided cardiac catheterization. Am J Physiol Heart Circ Physiol 2005;289(3):H1301-6.

61. Tzifa A, Polymerou I, Loggitsi D. Solely MRI-Guided Cardiac Catheterization for Assessment of Pulmonary Hypertension in a Pregnant Lady with Undiagnosed Congenital Heart Disease. Case Rep Cardiol 2020;2020:3072869.

62. Roos-Hesselink J, Baris L, Johnson M, De Backer J, Otto C, Marelli A, Jondeau G, Budts W, Grewal J, Sliwa K and others. Pregnancy outcomes in women with cardiovascular disease: evolving trends over 10 years in the ESC Registry Of Pregnancy And Cardiac disease (ROPAC). Eur Heart J 2019;40(47):3848-3855.

63. Velasco Forte MN, Roujol S, Ruijsink B, Valverde I, Duong P, Byrne N, Krueger S, Weiss S, Arar Y, Reddy SRV and others. MRI for Guided Right and Left Heart Cardiac Catheterization: A Prospective Study in Congenital Heart Disease. J Magn Reson Imaging 2021;53(5):1446-1457.

64. Elliott P, Arbustini E. The role of endomyocardial biopsy in the management of cardiovascular disease: a commentary on joint AHA/ACC/ESC guidelines. Heart 2009;95(9):759-60.

65. Leone O, Veinot JP, Angelini A, Baandrup UT, Basso C, Berry G, Bruneval P, Burke M, Butany J, Calabrese F and others. 2011 consensus statement on endomyocardial biopsy from the Association for European Cardiovascular Pathology and the Society for Cardiovascular Pathology. Cardiovasc Pathol 2012;21(4):245-74.

66. Rogers T, Ratnayaka K, Karmarkar P, Campbell-Washburn AE, Schenke WH, Mazal JR, Kocaturk O, Faranesh AZ, Lederman RJ. Real-time magnetic resonance imaging guidance improves the diagnostic yield of endomyocardial biopsy. JACC Basic Transl Sci 2016;1(5):376-383.

67. Sommer P, Grothoff M, Eitel C, Gaspar T, Piorkowski C, Gutberlet M, Hindricks G. Feasibility of real-time magnetic resonance imaging-guided electrophysiology studies in humans. Europace 2013;15(1):101-8.

68. Piorkowski C, Grothoff M, Gaspar T, Eitel C, Sommer P, Huo Y, John S, Gutberlet M, Hindricks G. Cavotricuspid isthmus ablation guided by real-time magnetic resonance imaging. Circ Arrhythm Electrophysiol 2013;6(1):e7-10.

69. Kholmovski EG, Coulombe N, Silvernagel J, Angel N, Parker D, Macleod R, Marrouche N, Ranjan R. Real-Time MRI-Guided Cardiac Cryo-Ablation: A Feasibility Study. J Cardiovasc Electrophysiol 2016;27(5):602-8.

70. Lichter J, Kholmovski EG, Coulombe N, Ghafoori E, Kamali R, MacLeod R, Ranjan R. Real-time magnetic resonance imaging-guided cryoablation of the

pulmonary veins with acute freeze-zone and chronic lesion assessment. Europace 2019;21(1):154-162.

71. Krueger JJ, Ewert P, Yilmaz S, Gelernter D, Peters B, Pietzner K, Bornstedt A, Schnackenburg B, Abdul-Khaliq H, Fleck E and others. Magnetic resonance imaging-guided balloon angioplasty of coarctation of the aorta: a pilot study. Circulation 2006;113(8):1093-100.

72. Oshinski JN, Parks WJ, Markou CP, Bergman HL, Larson BE, Ku DN, Mukundan S, Jr., Pettigrew RI. Improved measurement of pressure gradients in aortic coarctation by magnetic resonance imaging. J Am Coll Cardiol 1996;28(7):1818-26.

73. Schalla S, Saeed M, Higgins CB, Weber O, Martin A, Moore P. Balloon sizing and transcatheter closure of acute atrial septal defects guided by magnetic resonance fluoroscopy: assessment and validation in a large animal model. J Magn Reson Imaging 2005;21(3):204-11.

74. Strouse PJ, Beekman RH, 3rd. Magnetic deflection forces from atrial septal defect and patent ductus arteriosus-occluding devices, stents, and coils used in pediatric-aged patients. Am J Cardiol 1996;78(4):490-1.

75. Sharafuddin MJ, Gu X, Titus JL, Urness M, Cervera-Ceballos JJ, Amplatz K. Transvenous closure of secundum atrial septal defects: preliminary results with a new self-expanding nitinol prosthesis in a swine model. Circulation 1997;95(8):2162-8.

76. Buecker A, Spuentrup E, Grabitz R, Freudenthal F, Muehler EG, Schaeffter T, van Vaals JJ, Gunther RW. Magnetic resonance-guided placement of atrial septal closure device in animal model of patent foramen ovale. Circulation 2002;106(4):511-5.

77. Rickers C, Jerosch-Herold M, Hu X, Murthy N, Wang X, Kong H, Seethamraju RT, Weil J, Wilke NM. Magnetic resonance image-guided transcatheter closure of atrial septal defects. Circulation 2003;107(1):132-8.

78. Kort HW, Balzer DT, Johnson MC. Resolution of right heart enlargement after closure of secundum atrial septal defect with transcatheter technique. J Am Coll Cardiol 2001;38(5):1528-32.

79. Ratnayaka K, Saikus CE, Faranesh AZ, Bell JA, Barbash IM, Kocaturk O, Reyes CA, Sonmez M, Schenke WH, Wright VJ and others. Closed-chest transthoracic magnetic resonance imaging-guided ventricular septal defect closure in swine. JACC Cardiovasc Interv 2011;4(12):1326-34.

80. Halabi M, Faranesh AZ, Schenke WH, Wright VJ, Hansen MS, Saikus CE, Kocaturk O, Lederman RJ, Ratnayaka K. Real-time cardiovascular magnetic resonance subxiphoid pericardial access and pericardiocentesis using off-the-shelf devices in swine. J Cardiovasc Magn Reson 2013;15(1):61.

81. Arepally A, Karmarkar PV, Weiss C, Rodriguez ER, Lederman RJ, Atalar E. Magnetic resonance image-guided trans-septal puncture in a swine heart. J Magn Reson Imaging 2005;21(4):463-7.

82. Spuentrup E, Ruebben A, Schaeffter T, Manning WJ, Gunther RW, Buecker A. Magnetic resonance--guided coronary artery stent placement in a swine model. Circulation 2002;105(7):874-9.

83. Rogers T, Lederman RJ. Interventional CMR: Clinical applications and future directions. Curr Cardiol Rep 2015;17(5):31.

84. Schmidt EJ, Watkins RD, Zviman MM, Guttman MA, Wang W, Halperin HA. A Magnetic Resonance Imaging-Conditional External Cardiac Defibrillator for Resuscitation Within the Magnetic Resonance Imaging Scanner Bore. Circ Cardiovasc Imaging 2016;9(10).

85. Konings MK, Bartels LW, Smits HF, Bakker CJ. Heating around intravascular guidewires by resonating RF waves. J Magn Reson Imaging 2000;12(1):79-85.

86. Yildirim KD, Basar B, Campbell-Washburn AE, Herzka DA, Kocaturk O, Lederman RJ. A cardiovascular magnetic resonance (CMR) safe metal braided catheter design for interventional CMR at 1.5 T: freedom from radiofrequency induced heating and preserved mechanical performance. J Cardiovasc Magn Reson 2019;21(1):16.

87. Campbell-Washburn AE, Rogers T, Stine AM, Khan JM, Ramasawmy R, Schenke WH, McGuirt DR, Mazal JR, Grant LP, Grant EK and others. Right heart catheterization using metallic guidewires and low SAR cardiovascular magnetic

resonance fluoroscopy at 1.5 Tesla: first in human experience. J Cardiovasc Magn Reson 2018;20(1):41.

88. Kipling M, Mohammed A, Medding RN. Guidewires in clinical practice: applications and troubleshooting. Expert Rev Med Devices 2009;6(2):187-95.

89. Basar B, Rogers T, Ratnayaka K, Campbell-Washburn AE, Mazal JR, Schenke WH, Sonmez M, Faranesh AZ, Lederman RJ, Kocaturk O. Segmented nitinol guidewires with stiffness-matched connectors for cardiovascular magnetic resonance catheterization: preserved mechanical performance and freedom from heating. J Cardiovasc Magn Reson 2015;17:105.

90. Massmann A, Buecker A, Schneider GK. Glass-Fiber-based MR-safe Guidewire for MR Imaging-guided Endovascular Interventions: In Vitro and Preclinical in Vivo Feasibility Study. Radiology 2017;284(2):541-551.

91. Li X, Perotti LE, Martinez JA, Duarte-Vogel SM, Ennis DB, Wu HH. Real-time 3T MRI-guided cardiovascular catheterization in a porcine model using a glass-fiber epoxy-based guidewire. PLoS One 2020;15(2):e0229711.

92. Buecker A, Spuentrup E, Schmitz-Rode T, Kinzel S, Pfeffer J, Hohl C, van Vaals JJ, Gunther RW. Use of a nonmetallic guide wire for magnetic resonance-guided coronary artery catheterization. Invest Radiol 2004;39(11):656-60.

93. Serfaty JM, Yang X, Aksit P, Quick HH, Solaiyappan M, Atalar E. Toward MRI-guided coronary catheterization: visualization of guiding catheters, guidewires, and anatomy in real time. J Magn Reson Imaging 2000;12(4):590-4.

94. Brecher C, Emonts M, Brack A, Wasiak C, Schutte A, Kramer N, Bruhn R. New concepts and materials for the manufacturing of MR-compatible guide wires. Biomed Tech (Berl) 2014;59(2):147-51.

95. Campbell-Washburn AE, Rogers T, Basar B, Sonmez M, Kocaturk O, Lederman RJ, Hansen MS, Faranesh AZ. Positive contrast spiral imaging for visualization of commercial nitinol guidewires with reduced heating. J Cardiovasc Magn Reson 2015;17:114.

96. Ratnayaka K, Rogers T, Schenke WH, Mazal JR, Chen MY, Sonmez M, Hansen MS, Kocaturk O, Faranesh AZ, Lederman RJ. Magnetic Resonance

Imaging-Guided Transcatheter Cavopulmonary Shunt. JACC Cardiovasc Interv 2016;9(9):959-70.

97. Greer JS, Hussein MA, Vamsee R, Arar Y, Krueger S, Weiss S, Dillenbeck J, Greil G, Veeram Reddy SR, Hussain T. Improved catheter tracking during cardiovascular magnetic resonance-guided cardiac catheterization using overlay visualization. J Cardiovasc Magn Reson 2022;24(1):32.

98. Neofytou AP, Kowalik GT, Vidya Shankar R, Huang L, Moon T, Mellor N, Razavi R, Neji R, Pushparajah K, Roujol S. Automatic image-based tracking of gadolinium-filled balloon wedge catheters for MRI-guided cardiac catheterization using deep learning. Front Cardiovasc Med 2023;10:1233093.

99. Doorey AJ, Turi ZG, Lazzara EH, Casey M, Kolm P, Garratt KN, Weintraub WS. Safety gaps in medical team communication: Closing the loop on quality improvement efforts in the cardiac catheterization lab. Catheter Cardiovasc Interv 2022;99(7):1953-1962.

100. Nakanishi T. Cardiac catheterization is necessary before bidirectional Glenn and Fontan procedures in single ventricle physiology. Pediatr Cardiol 2005;26(2):159-61.

101. Mohammad Nijres B, Murphy JJ, Diab K, Awad S, Abdulla RI. Routine Cardiac Catheterization Prior to Fontan Operation: Is It a Necessity? Pediatr Cardiol 2018;39(4):818-823.

102. Guruchandrasekar SH, Dakin H, Kadochi M, Bhatia A, Bardales L, Johnston M, Piggott KD. Pre-Fontan Cardiac Catheterization Data as a Predictor of Prolonged Hospital Stay and Post-Discharge Adverse Outcomes Following the Fontan Procedure: A Single-Center Study. Pediatr Cardiol 2020;41(8):1697-1703.

103. Eilers LF, Britt JJ, Weigand J, Penny DJ, Gowda ST, Qureshi AM, Stapleton GE, Khan A, Webb MK, Bansal M. Pre-Fontan Assessment Utilizing Combined Cardiac Catheterization and Cardiac MRI: Comparison to the Pre-Fontan Catheterization. Pediatr Cardiol 2024;45(7):1448-1454.

104. Campbell-Washburn AE, Ramasawmy R, Restivo MC, Bhattacharya I, Basar B, Herzka DA, Hansen MS, Rogers T, Bandettini WP, McGuirt DR and others. Opportunities in Interventional and Diagnostic Imaging by Using High-Performance Low-Field-Strength MRI. Radiology 2019;293(2):384-393.

105. Rogers T, Ratnayaka K, Schenke WH, Sonmez M, Kocaturk O, Mazal JR, Chen MY, Flugelman MY, Troendle JF, Faranesh AZ and others. Fully percutaneous transthoracic left atrial entry and closure as a potential access route for transcatheter mitral valve interventions. Circ Cardiovasc Interv 2015;8(6):e002538.

106. Fisher DL. The use of pressure recordings obtained at transthoracic left heart catheterization in the diagnosis of valvular heart disease. J Thorac Surg 1955;30(4):379-92.

107. Rahman NM, Ali NJ, Brown G, Chapman SJ, Davies RJ, Downer NJ, Gleeson FV, Howes TQ, Treasure T, Singh S and others. Local anaesthetic thoracoscopy: British Thoracic Society Pleural Disease Guideline 2010. Thorax 2010;65 Suppl 2:ii54-60.

108. Schmitt B, Sabi TM, Sigler M, Berger F, Ewert P. Upper cavo-pulmonary anastomosis by transcatheter technique. Catheter Cardiovasc Interv 2012;80(1):93-9.

109. Ratnayaka K, Moore JW, Rios R, Lederman RJ, Hegde SR, El-Said HG. First-in-Human Closed-Chest Transcatheter Superior Cavopulmonary Anastomosis. J Am Coll Cardiol 2017;70(6):745-752.

110. Kuehne T, Yilmaz S, Steendijk P, Moore P, Groenink M, Saaed M, Weber O, Higgins CB, Ewert P, Fleck E and others. Magnetic resonance imaging analysis of right ventricular pressure-volume loops: in vivo validation and clinical application in patients with pulmonary hypertension. Circulation 2004;110(14):2010-6.

111. Barber NJ, Ako EO, Kowalik GT, Cheang MH, Pandya B, Steeden JA, Moledina S, Muthurangu V. Magnetic Resonance-Augmented Cardiopulmonary Exercise Testing: Comprehensively Assessing Exercise Intolerance in Children With Cardiovascular Disease. Circ Cardiovasc Imaging 2016;9(12)